

**PHENOL REMOVAL WITH ELECTROCHEMICAL  
CARBON NANOTUBES FILTER COUPLED WITH IN  
SITU GENERATED H<sub>2</sub>O<sub>2</sub>**

**XIA QING**

(B. Eng., Peking University)

**A THESIS SUBMITTED**

**FOR THE DEGREE OF MASTER OF SCIENCE**

**DEPARTMENT OF CHIMISTRY**

**NATIONAL UNIVERSITY OF SINGAPORE**

**2014**

## DECLARATION

I hereby declare that this thesis is my original work and it has been written by me in its entirety, under the supervision of Prof. Sam Li, co-supervision of Prof. Zhi ZHOU, (in the laboratory Environmental Biotechnology), Chemistry Department, National University of Singapore, between 04 August 2013 and 04 August 2014.

I have duly acknowledged all the sources of information which have been used in the thesis.

This thesis has also not been submitted for any degree in any university previously.

Xia Qing

---

Name



---

Signature

10 December 2014

---

Date

## **ACKNOWLEDGEMENT**

This work is supported by the Singapore National Research Foundation under its Environment and Water Technologies Strategic Research Programme and administered by the Environment and Water Industry Programme Office (EWI) of the PUB on project 1102-IRIS-14-03.

# TABLE OF CONTENTS

<b>DECLARATION.....</b>	<b>I</b>
<b>ACKNOWLEDGEMENT.....</b>	<b>II</b>
<b>SUMMARY .....</b>	<b>V</b>
<b>LIST OF TABLES .....</b>	<b>VI</b>
<b>LIST OF FIGURES .....</b>	<b>VII</b>
<b>1 INTRODUCTION.....</b>	<b>1</b>
1.1 Background.....	1
1.2 Carbon nanotubes.....	3
1.3 Hydrogen peroxide electrogeneration.....	6
1.4 Justification of the research project .....	8
1.5 Objectives .....	8
1.6 Scope.....	9
<b>2 LITERATURE REVIEW .....</b>	<b>10</b>
2.1 Contaminants in wastewater treatment .....	10
2.2 Carbon nanotubes in water treatment .....	11
2.3 Hydrogen peroxide electrogeneration for water treatment .....	14
2.3.1 Cathode materials .....	15
2.3.2 Divided reactors .....	17
2.3.3 Undivided reactors .....	17
2.4 Phenol removal and oxidation .....	19
2.4.1 Removal methods for phenol .....	19
2.4.2 Oxidation products of phenol.....	20
<b>3 MATERIALS AND METHODS .....</b>	<b>21</b>
3.1 Chemicals and materials .....	21
3.2 Electrochemical carbon nanotubes filter preparation .....	21
3.3 Carbon nanotube surface treatment .....	22
3.4 Electrochemical filtration apparatus and characterization.....	22
3.5 Characterization of carbon nanotubes filters .....	23
3.6 pH and dissolved oxygen analysis. ....	24
3.7 Hydrogen peroxide determination method .....	24
3.8 Phenol, Methyl orange, tetracycline, geosmin and MIB determination method.....	25

<b>4</b>	<b>HYDROGEN PEROXIDE PRODUCTION WITH ELECTROCHEMICAL CARBON NANOTUBES SYSTEM.....</b>	<b>26</b>
4.1	Cyclic voltammetry.....	26
4.2	Comparison of electro-generation of H <sub>2</sub> O <sub>2</sub> in solutions with different pH values .....	27
4.3	Comparison of electro-generation of H <sub>2</sub> O <sub>2</sub> with different dissolved oxygen .....	29
4.4	Electro-generation of H <sub>2</sub> O <sub>2</sub> with different flow rate.....	30
4.5	Electro-generation of H <sub>2</sub> O <sub>2</sub> with different grade CNT membranes.....	32
4.6	Electro-generation of H <sub>2</sub> O <sub>2</sub> with different treatment process .....	34
4.7	Comparison of titanium and CNT cathodes.....	36
4.8	Effects of cathode potential on electrochemical and effluent characteristics .....	37
<b>5</b>	<b>PHENOL OXIDATION BY H<sub>2</sub>O<sub>2</sub> WITH ELECTROCHEMICAL CARBON NANOTUBES FILTER .....</b>	<b>47</b>
5.1	Introduction of Aqueous aromatic compounds and phenol .....	47
5.2	Statistic batch experiment for phenol removal .....	48
5.3	Phenol oxidation with different influent concentrations.....	49
5.4	Phenol oxidation with different DO concentrations .....	52
5.5	Effects of different flow rate.....	53
5.6	Phenol oxidation with different grades membranes.....	54
5.7	Effects of membranes with different treatments .....	55
5.8	Effects of other reactive oxygen species.....	56
5.9	Phenol removal effect in long term.....	58
<b>6</b>	<b>ENERGY EFFICIENCY AND APPLICATION FOR THE ELECTROCHEMICAL CARBON NANOTUBES FILTER SYSTEM..</b>	<b>60</b>
6.1	Energy consumption for electrochemical phenol filtration .....	60
6.2	Oxidation of other organic contaminants.....	61
<b>7</b>	<b>CONCLUSIONS AND RECOMMENDATIONS.....</b>	<b>63</b>
7.1	Conclusions.....	63
7.2	Recommendations.....	64
<b>8</b>	<b>BIBLIOGRAPHY .....</b>	<b>65</b>

## SUMMARY

Electrochemically active carbon nanotube (CNT) filters can effectively adsorb and oxidize certain compounds in the anode, but the role of a cathode in electrochemical filters beyond a counter electrode has not been thoroughly investigated. In this study, a new wastewater treatment system combining adsorption and oxidation in the CNT anode and oxidation with *in situ* generated hydrogen peroxide ( $\text{H}_2\text{O}_2$ ) in the CNT cathode was developed. The treatment efficiency, impacting factors, and mechanism of the system were systematically studied. The results demonstrate that electrode material, cathode potential, pH, flow rate, and dissolved oxygen (DO) could affect  $\text{H}_2\text{O}_2$  yield. The maximum  $\text{H}_2\text{O}_2$  yield of  $1.38 \text{ mol hr}^{-1} \text{ m}^{-2}$  was achieved with C-grade CNT at an applied cathode potential of  $-0.4 \text{ V}$  (vs. Ag/AgCl), a pH of 6.46, a flow rate of  $1.5 \text{ mL min}^{-1}$ , and an influent DO of  $44 \text{ mg L}^{-1}$ . Phenol was used as a model aromatic compound to evaluate the removal efficiency and its oxidation rate was directly correlated with the  $\text{H}_2\text{O}_2$  yield. A high phenol removal efficiency of  $87.0 \pm 1.8\%$  within 4 h of continuous operation was achieved with an average oxidation rate of  $0.059 \pm 0.001 \text{ mol hr}^{-1} \text{ m}^{-2}$  at an applied cathode potential of  $-0.4 \text{ V}$  (vs. Ag/AgCl). Scavenger tests indicate that phenol oxidation was mainly due to electrogenerated  $\text{H}_2\text{O}_2$  and other reactive oxygen species (e.g.,  $\text{HO}_2^\bullet$ , and  $\text{O}_2^{\bullet-}$ ), but not hydroxyl radicals ( $\text{OH}^\bullet$ ). The newly developed electrochemical CNT filtration system coupled with *in situ* generated  $\text{H}_2\text{O}_2$  may be used as a cost-effective wastewater treatment system to remove organic pollutants or a promising point-of-use wastewater treatment system.

## LIST OF TABLES

Table 1-1. Physicochemical properties of hydrogen peroxide .....	7
Table 4-1. Dimension and BET for different grade carbon nanotubes .....	33
Table 5-1. Physicochemical properties of phenol (carbolic acid) .....	48

## LIST OF FIGURES

Figure 2-1. Catalytic oxidation reaction of phenol.....	20
Figure 3-1. Schematic diagram of electrochemical reactor.....	24
Figure 3-2. Calibration curve of phenol. ....	25
Figure 4-1. Cyclic voltammetry curves of the CNT electrochemical filter as a functional applied cathode potential and DO levels.....	27
Figure 4-2. Electrochemical H <sub>2</sub> O <sub>2</sub> yield as a function of pH .....	28
Figure 4-3. Electrochemical H <sub>2</sub> O <sub>2</sub> yield as a function of DO .....	30
Figure 4-4. Electrochemical H <sub>2</sub> O <sub>2</sub> yield as a function of flow rate.....	32
Figure 4-5. Electrochemical H <sub>2</sub> O <sub>2</sub> yield as a function of CNT dimensions.....	33
Figure 4-6. Production of H <sub>2</sub> O <sub>2</sub> with different treatment process .....	36
Figure 4-7. Effect of cathode materials on H <sub>2</sub> O <sub>2</sub> yield and phenol oxidation rate: comparison of titanium cathode and CNT cathode. ....	37
Figure 4-8. Steady-state current as a function of applied cathode potential .....	38
Figure 4-9. Applied voltage as a function of applied cathode potential.....	39
Figure 4-10. Applied voltage as a function of applied cathode potential.....	41
Figure 4-11. Bubbles generated at cathode at applied.....	41
Figure 4-12. Effluent DO concentration as a function of applied cathode potential .....	43
Figure 4-13. DO efficiency as a function of pH and applied cathode potential ....	44
Figure 4-14. Current Efficiency as a function of applied cathode potential .....	44
Figure 5-1. Absorbance of 50 mg L <sup>-1</sup> phenol solution at 0 h and 2 h after adding 33 mg L <sup>-1</sup> H <sub>2</sub> O <sub>2</sub> .....	48
Figure 5-2. Breakthrough curve of 50 mg L <sup>-1</sup> phenol. ....	49
Figure 5-3. Effect of influent phenol concentrations on phenol oxidation rate ....	50
Figure 5-4. Phenol removal experiment .....	52
Figure 5-5. TOC of phenol as a function of applied cathode potential. ....	52
Figure 5-6. Effect of DO on phenol oxidation rate .....	53
Figure 5-7. Removal efficiency of 50 mg L <sup>-1</sup> phenol and production of H <sub>2</sub> O <sub>2</sub> with different flow rate .....	54
Figure 5-8. Removal efficiency of 50 mg/L phenol with different grade CNT ....	55
Figure 5-9. Removal efficiency of 50 mg/L phenol with different treatment process .....	56
Figure 5-10. Effect of benzoquinone on phenol oxidation rate.....	57
Figure 5-11. Effect of <i>tert</i> -butanol on phenol oxidation rate .....	58
Figure 5-12. FESEM images of (a) cathodic and (b) anodic CNT filters after 4 h continuous phenol oxidation, showing some polymerization on CNT surface.....	59
Figure 5-13. Phenol oxidation rate and current as a function of time .....	59
Figure 6-1. Comparison of removal efficiency of 0.1 mmol L <sup>-1</sup> tetracycline, .....	62



# 1 INTRODUCTION

## 1.1 Background

Water is essential for the subsistence of living beings and is a critical factor in ecological balance. Although its volume (~1400 million km<sup>3</sup>) on earth is abundant, the majority of it is constituted by saltwater and only 2.5% of freshwater is readily available for human uses (Oki & Kanae, 2006). With developments of economics and industry, water pollution threatens the safety of drinking water and human health (Vorosmarty *et al.*, 2010). Various kinds and great quantity of contaminants were released into water bodies could accumulate in wild animals and human being. It is well known that large amounts of synthetic organic pollutants, including industrial chemicals, pesticides, dyes and pharmaceuticals and personal care products (PPCPs), are released daily into many types of wastewaters and enter into natural water bodies. Conventional regulations only focus on pathogens and parasites, nutrients, priority pollutants, refractory organics, heavy metals, and dissolved inorganics etc. Emerging contaminants not in the list of conventional regulations, include artificial sweeteners (sucralose), nanomaterials, perfluorinated compounds (PFCs), pharmaceuticals, hormones, drinking water disinfection byproducts (DBPs), sunscreens/UV filters, brominated flame retardants, benzotriazoles, naphthenic acids, antimony, siloxanes, musks, algal toxins, and pesticide transformation products (Richardson & Ternes, 2011). These emerging contaminants are used

in small quantities by millions of people in many locations, but may add up to much impact on the environment.

Chemical contaminants may have a harmful effect on living organisms or make water unsuitable for desired use. In our daily necessities, some products contain significant amounts of contaminants, such as phthalate esters (a kind of industrial compound that makes PVC toys soft and pliable – *plasticizers*, some of them were supposed endocrine disruptors) in plastic toys, ethynyl estradiol in pharmaceuticals, methoxychlor in industrial chemicals, cimetidine in drugs for birth control and diethylstilbestrol given to mothers to prevent morning sickness (Calle *et al.*, 1996; Sanderson *et al.*, 1998). These contaminants might enrich in wild animals and human bodies through natural water and lead to reproductive disorders, immune system dysfunction, certain cancers, birth defects and falling sperm counts, neurological effects, attention deficit disorder and poor memory, and low IQ (Schwarzenbach *et al.*, 2010). Negative effects of contaminants on wild animals have been widely reported: 700 bottle nose dolphins died along the coasts of New Jersey and Florida (Geraci, 1989), 20,000 harbour seals died within a few months in the North Sea (Dietz *et al.*, 1989), and negative effects on amphibian deformities (Taylor *et al.*, 2005). For human beings, waterborne diseases like diarrheal caused by over 20 viral, bacterial and parasitic infections are responsible for 2 to 2.5 million deaths annually. In developing countries, the persistent organic pollution emissions have been increasing greatly due to the increasing energy demand associated with rapid population growth and

economic development and to the low efficiency of energy utilization (Xu *et al.*, 2013).

Besides the water contaminants mentioned above, large amount of emerging water pollution is generated with industrial development. In order to prevent from human health disorder and ecosystem unbalance, some activities must be taken to relieve water pollution and remove those aqueous contaminants from water body. This study focuses on an innovative process to remove and oxidize one aqueous organic product, phenol, with electrogenerated hydrogen peroxide from carbon nanotubes cathode.

## **1.2 Carbon nanotubes**

Carbon nanotubes was discovered in 1991, and they have been applied in most areas of science and engineering and generated huge unprecedented results and effects due to their special physical and chemical properties. These superlative mechanical, electronic properties, and thermal conductivity make carbon nanotubes ideal for a wide range of applications in materials of carbon nanotubes in some baseball bats, golf clubs or car parts (Baughman *et al.*, 2002), fundamental research, water treatment, and material science (Cao *et al.*, 2004).

Carbon nanotubes are allotropes of carbon with a cylindrical nanostructure. Their unique strength attribute to the chemical bonding composed entirely of  $sp^2$  bonds, similar to those of graphite, which are stronger than the  $sp^3$  bonds found in alkanes and diamond. Two main types of nanotubes are used mostly, single-walled carbon nanotube (SWNT) (Bethune *et al.*, 1993) and multi-walled carbon nanotube (MWNT) (Iijima & Ichihashi, 1993). The former consists of a single

sheet of graphene rolled seamlessly to form a cylinder with diameter of order of 1 nm and length of up to centimeters, while the latter, MWNT, consist of an array of such cylinders formed concentrically and separated by 0.35 nm, similar to the basal plane separation in graphite (Iijima, 1991). The synthetic processes are based on arc discharge, laser ablation, plasma torch, chemical vapor deposition (CVD), super-growth CVD, and removal of catalysts and decomposition of CO. Because there are many possibilities for the relationship between axial direction and unit vectors for hexagonal lattice, carbon nanotubes could be metallic, semi-metallic or semi-conducting (Coleman *et al.*, 2006). Pristine carbon nanotubes are extremely conductive due to almost hardly scattering effects in ballistic transport from the one-dimensional structure. Even superconductivity was observed in SWNT at transition temperature around 5 K (Tang *et al.*, 2001). Besides unique electrical features, the physical characteristics of carbon nanotubes attract scientists' attention as well. The size of carbon nanotubes can be made into extremely tiny particles. The shortest carbon nanotube is the organic compound cycloparaphenylene, which was synthesized in early 2009 by Lawrence Berkeley National Laboratory; the thinnest carbon nanotube is only 3 Å diameter with armchair (2,2) which was grown inside a MWNT (Zhao *et al.*, 2004). In spite of the tiny dimension and size, the physical strength of carbon nanotubes is extremely high due to its C-C bonds. The tensile strength of carbon nanotubes was still not accurately measured. However the estimation on strength from properties of C-C bonds was as high as 130 GPa (Cottrell, 1964), for fabricated graphite whiskers, the tensile strength was around 20 GPa (Bacon,

2004). Other studies showed individual carbon nanotube shells have strengths of up to over 100 GPa, which is in agreement with quantum and atomistic models (Peng *et al.*, 2008). For the strong covalent  $sp^2$  bonds formed between the individual carbon atoms, since the density for a solid CNT is as low as 1.3 to 1.4  $g/cm^3$ , CNT has the best specific strength known till now, up to 48,000  $kN\ m\ kg^{-1}$ , compared to 154  $kN\ m\ kg^{-1}$  for high-carbon steel (Collins & Avouris, 2000). The tensile strength of carbon nanotube is extremely high, while the shear interaction between adjacent shells and tubes is too weak due to its large length and width ratio. Standard SWNT could withstand a pressure up to 25 GPa without deformation. For higher pressure, it will be transformed into a harder phase, which could withstand 55 GPa (Popov *et al.*, 2002). Because of the symmetry and unique electronic structure of graphene, the structure of a nanotube strongly affects its electrical properties. In theory, metallic nanotubes can carry an electric current density of  $4 \times 10^9 A/cm^2$ , which is more than 1,000 times greater than those of metals such as copper, whose current densities are limited by electromigration (Hong & Myung, 2007). Along tubes, all nanotubes are good thermal conductors. Measurements show that the thermal conductivity along the axis of single-walled carbon nanotubes is  $3500\ W\ m^{-1}\ K^{-1}$  at room temperature (Pop *et al.*, 2006) while copper transmits thermal at the rate of only  $385\ W\ m^{-1}\ K^{-1}$ . The thermal conductivity across its axis is about  $1.52\ W\ m^{-1}\ K^{-1}$  and close to that of soil. CNT also shows stability at high temperature up to  $2800\ ^\circ C$  in vacuum, or  $750\ ^\circ C$  in air (Thostenson *et al.*, 2005).

Considering the superlative tensile physical mechanical characteristics, electronic properties, thermal conductivity and other features, carbon nanotubes have huge potential applications in both industrial manufacture and science researches. Restricted to the synthesis of carbon nanotubes, current applications are mostly limited to the use of bulk nanotubes because only unorganized fragments of bulk nanotubes could be batch manufactured. Carbon nanotubes are used as tips for atomic force microscope for its high length-width ratio dimension and excellent electromigration ability (Hafner *et al.*, 2001). In tissue engineering, it acts a role as scaffolding for bone growth (Zanello *et al.*, 2006). MWNT also could be made into filters for viral and bacterial inactivation (Vecitis *et al.*, 2011).

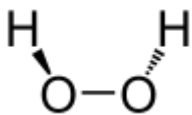
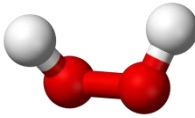
### **1.3 Hydrogen peroxide electrogeneration**

Hydrogen peroxide ( $H_2O_2$ ) is a potential strong oxidant as an environmentally friendly chemical because no hazardous residuals were left after reaction except oxygen and water.  $H_2O_2$  is a colorless liquid with little blue color. Due to its high oxidation properties,  $H_2O_2$  is often applied to bleaching of paper pulp, treatment of wastewater, cleaning agent and destruction of hazardous organic wastes (Qiang *et al.*, 2002). The physicochemical properties of hydrogen peroxide are listed in Table 1-1.

In the environmental field,  $H_2O_2$  is used as a supplement of oxygen source to enhance the bioremediation of contaminated aquifers (Wilson *et al.*, 1994). It is used for cleaning well water or other drinking water sources, by removing odors, organic materials that change the water taste, and the removal of  $H_2S$  and iron, while reducing trihalomethanes and haloacetic acids. Hydrogen peroxide

can be used to increase or decrease the amount of ozone in drinking water. H<sub>2</sub>O<sub>2</sub> is a conventional oxidant to reduce BOD and COD of industrial wastewater for many years. High concentration H<sub>2</sub>O<sub>2</sub> is referred to as high test peroxide, used as rocket propellant. H<sub>2</sub>O<sub>2</sub> could generate another stronger oxidant, hydroxyl radical (OH·), with Fe<sup>2+</sup>, which produces the Fenton's reagent for either degradation or synthesis of organic compounds (Scialdone *et al.*, 2013). However, the Fenton system needs extra chemicals and energy to continuously generate hydroxyl radicals. What's more, the residuals of Fenton system and ferrous/ferric ions in treated water still need to be solved.

**Table 1-1. Physicochemical properties of hydrogen peroxide**

	Properties
Chemical name	Hydrogen peroxide
Molecular formula	H <sub>2</sub> O <sub>2</sub>
Chemical structure	 
Molecular weight	34.0147 g mol <sup>-1</sup>
Class	Oxidant, Corrosive

H<sub>2</sub>O<sub>2</sub> can be produced by electrochemical methods, such as electrolysis of inorganic chemicals (H<sub>2</sub>S<sub>2</sub>O<sub>8</sub>, KHSO<sub>4</sub> and NH<sub>4</sub>HSO<sub>4</sub>) and autoxidation of organic compounds (alkylhydroanthraquinones and isopropyl alcohol). The electrolysis process of inorganics needs large amount of energy and chemicals. Hydrogen peroxide could be directly generated from water with thermal, photochemical, and electrical discharge processes although it requires demanding operational conditions.

Although H<sub>2</sub>O<sub>2</sub> is a strong oxidant, low concentrations (~3%) of H<sub>2</sub>O<sub>2</sub>, are widely available and legal to buy for medical use according to many regulations.

#### **1.4 Justification of the research project**

Large amounts of organic wastes discharged into water bodies have caused serious water pollutions that substantially damaged the aquatic environments (Liu *et al.*, 2011). Therefore, effective approaches to remove these pollutants are highly desirable. An electrochemically active multi-walled carbon nanotubes (MWNTs) filter has been previously proven to be effective toward the adsorptive removal and anodic oxidation of certain selected compounds (Liu *et al.*, 2012). However, the role of a cathode of the electrochemical filter beyond a counter electrode is usually disregarded.

Oxidation and removal of these pollutants with electrogenerated hydrogen peroxide in two-MWNT-membrane filter system is an innovative process. Considering the environmental friendly feature of H<sub>2</sub>O<sub>2</sub>, its residuals and byproducts, oxygen and water, would not pollute water. Through adjustment and optimization for conditions applied on the carbon nanotube filter system, on-site continuous hydrogen peroxide could be generated from water without extra chemicals except oxygen pumped into water.

#### **1.5 Objectives**

In this work, the *in-situ* production of strong oxidation species, e.g. hydrogen peroxide (H<sub>2</sub>O<sub>2</sub>), at the functional CNT cathode within the electrochemical filter was systematically studied. The objective of this study was



to develop a novel wastewater treatment system combining adsorption and oxidation in the CNT anode and oxidation with *in situ* generated hydrogen peroxide ( $H_2O_2$ ) in the CNT cathode. A series of control experiments were conducted on MWNTs to optimize conditions for hydrogen peroxide ( $H_2O_2$ ) generation in electrochemical carbon nanotubes filters, including cathode potential, flow rate, influent pH value, concentration of dissolved oxygen, dimension of WMNT and preparation treatment. Aqueous organic products such as phenol were oxidized and removed from the water with hydrogen peroxide in electrochemical carbon nanotube system, and its performance and oxidation rate was correlated with  $H_2O_2$  production rate.

## **1.6 Scope**

In this study, an innovative wastewater treatment process with electrochemical carbon nanotubes filtration was studied. With the technology, aqueous organic products in waste water were removed by absorption and oxidation. Hydrogen peroxide was generated at low cathode potential from reaction on CNT membranes. As a green oxidant,  $H_2O_2$  could remove phenol and other aqueous organic products without DBPs. Low energy consumption was needed with this technology for water treatment.

## 2 LITERATURE REVIEW

### 2.1 Contaminants in wastewater treatment

With the rapid increase in population and fast industrial development in recent decades, large amounts of organic wastes discharged into water bodies have caused serious water pollutions that substantially damaged the aquatic environments (Liu *et al.*, 2011). Water systems are transformed through widespread land cover change, urbanization, industrialization and engineering schemes like reservoirs, irrigation and interbasin transfers that maximize human access to water (Programme, 2009). However on the other aspect, nearly 80% (4.8 billion) of the world's population (for 2000) lives in areas where either incident human water security or biodiversity threat exceeds the 75th percentile (Vorosmarty *et al.*, 2010). Over 30 of the 47 largest rivers, which collectively discharge half of global runoff to the oceans, show at least moderate threat levels (incident biodiversity threat index  $> 0.5$ ) at river mouth, with eight rivers (for human water security) and fourteen (for biodiversity) showing very high threat (incident biodiversity threat index  $> 0.75$ ). Mining, agricultural, urban and industrial activities contribute large contaminant loads to water body, including organic chemicals, heavy metals and sediment (Programme, 2009). Over 300 chemicals from a diverse range of classes of compounds have been identified in wastewater. Their concentrations vary from the  $\text{pg kg}^{-1}$  to  $\text{g kg}^{-1}$  range, depending on the type of wastewater, domestic, municipal or industrial (Jacobs *et al.*, 1987; Smith, 2000). Some most frequently detected contaminants include aromatics, polycyclic aromatic hydrocarbons (PAHs), polychlorinated biphenyls (PCBs),

phthalic acid esters (PAEs), polychlorinated dibenzo-*p*-dioxins and furans (PCDD/Fs), organochlorinated pesticides and phenols (Dai *et al.*, 2007; Harrison *et al.*, 2006). In America's streams, 80% of the samples from streams detected with organic wastewater contaminants (OWCs), which represent a wide range of residential, industrial and agricultural origins and uses with 82 OWCs (Kolpin *et al.*, 2002). More and more water body will be polluted with speedily development of modern industry and medical products. And with more precise analytical technologies in the future, more emerging contaminants in water will definitely be found and attract scientists' attentions. Therefore, seeking effective approaches that can remove these pollutants to non-hazardous products are highly desirable.

In this study, phenol was selected as a target emerging contaminant in wastewater not only because its aqueous form is toxic and refractory to conventional biological wastewater treatment, but also because it is frequently used as a model aromatic compound in industrial wastewater treatment studies as millions of tons of phenol are produced in every year.

## **2.2 Carbon nanotubes in water treatment**

Recent advances in membrane technology have led to an increased use of synthetic organic/inorganic membranes for water treatment including the removal of viruses and hazardous chemicals from contaminated sources of water (Lewis *et al.*, 2011). Among all the promising membrane materials, carbon nanotubes have attracted extensive attention due to their combination of mechanical stability, flexibility and chemical resistivity and large specific

surface area, and were considered as a good option for membrane materials (Iijima, 1991; Pan & Xing, 2008; Yang *et al.*, 2013). CNT can also be easily formed into porous 3D networks that can be used as filters for contaminant sorption and electrochemical degradation due to their specific surface area (30-650 m<sup>2</sup> g<sup>-1</sup>) (Lee *et al.*, 2005) and conductivity (around 10<sup>4</sup>~10<sup>6</sup> S·m<sup>-1</sup>) (Ma *et al.*, 1999). Previous results have demonstrated that the CNT-based electrochemical filters proven to be effective to adsorb and anodic oxidize aqueous organic pollutants, such as azo dyes and phenol (Gao & Vecitis, 2011; Vecitis *et al.*, 2011b; Rahaman *et al.*, 2012). Within the electrochemical CNT filtration system, organic pollutants were adsorbed and oxidized via a direct/indirect oxidation process on the anodic CNT filters,(Liu & Vecitis, 2012) and a Ti ring or CNT filters were used as a counter cathode to provide the required potential (Schnoor & Vecitis, 2013; Vecitis *et al.*, 2011a). However, the role of a cathode in electrochemical filters beyond a counter electrode has not been thoroughly investigated, as previous studies mainly focus on the anodic oxidation of organic pollutions (Gao & Vecitis, 2011; Vecitis *et al.*, 2011a).

Integrated electrochemical technologies that combine pressure driven CNT membrane processes with EAOPs have been gaining attention recently. The enhanced performance of three-dimensional electrodes arose from the high surface area increasing the number of electrochemically active surface sites (Cinke *et al.*, 2002) and high porosity for enhanced ion and molecular transport. High pressure CNT membranes may provide an effective treatment barrier to isolate most trace organic and inorganic compounds and microorganisms,

although adsorption, size exclusion and charge repulsion have a major influence on the treatment efficiency (Sirés & Brillas, 2012). CNT network was utilized as an anodic water filter and shown to be effective for some aromatic dye, e.g., methylene blue and methyl orange, and anion, e.g., chloride and iodide removal and oxidation (Gao & Vecitis, 2011) and bacterial and virus removal and inactivation (Vecitis *et al.*, 2011). CNT doping with boron or nitrogen had been shown to affect the CNT electronic structure and in turn will likely also enhance the electrochemistry activity of CNT. With such doped CNT networks, 50% of 0.2 mmol L<sup>-1</sup> phenol was able to be removed from influent water (Gao & Vecitis, 2012). Some pretreatments on CNT, e.g. calcination, redispersion in HCl, toluene and hexanes, were efficient to improve the removal effect of passivating electro polymer coating (Gao & Vecitis, 2013). Carbon nanotube filtration worked well toward pharmaceuticals in drinking water treatment plant, over 85% rejection percentages (Radjenović *et al.*, 2008). Electrochemical oxidation for diclofenac and ibuprofen from yellow waters in membrane system in a batch plant was useful, destroying both compounds without loss of urea as a nitrogen fertilizer (Lazarova *et al.*, 2008).

Until now, in most of the studies, the anodic CNT was prepared by a facile vacuum filtration of CNT dispersions and a Ti ring or another CNT filters was served as a cathode within the electrochemical CNT filters. Upon application of a certain anodic potential, the target compounds can be not only adsorbed onto the anodic CNT filters but also partially or completely oxidized via a direct/indirect oxidation process on the anodic CNT filters (Liu & Vecitis, 2012).

They mainly focused on the anodic oxidation of organic pollutions at the anode (Gao & Vecitis, 2011; Vecitis *et al.*, 2011b), the role of a cathode of the electrochemical filter beyond a counter electrode is usually disregarded within this kind of electrochemical setup. In fact, the *in-situ* production of strong oxidation species, e.g. hydrogen peroxide (H<sub>2</sub>O<sub>2</sub>), can be achieved via a two electron oxygen reduction reaction (Eq. 1) once the counter electrode was served as a functional cathode (Brillas *et al.*, 2009b; Hsiao & Nobe, 1993; Pignatello *et al.*, 2006a; Xie & Li, 2006).



This work investigated the cathodic oxidation and removal effect for organic products, here taking phenol as the target product. Its hydrogen peroxide production on cathode CNT membrane and relevant influent factors analysed as well.

### **2.3 Hydrogen peroxide electrogeneration for water treatment**

Hydrogen peroxide is a “green” chemical for the oxidization of various organic pollutants that leaves oxygen and water as by-products (Forti *et al.*, 2007; Guillet *et al.*, 2006; Isarain-Chávez *et al.*, 2013; Yuan *et al.*, 2011) as well as a strong oxidant (E<sub>0</sub>=1.763 V vs. Standard Hydrogen Electrode” (SHE)) (E. Brillas *et al.*, 2009b). It is also one of the most essential chemicals for pulp bleaching, electronic circuits cleaning, medical disinfection, wastewater treatment and chemical production (Pletcher, 1999). In the environmental field, hydrogen peroxide is used as a supplement of oxygen source to enhance the bioremediation

of contaminated aquifers (Wilson *et al.*, 1994). Coupled with ozone or UV radiation, H<sub>2</sub>O<sub>2</sub> could decompose aqueous organic contaminants effectively (Bellamy *et al.*, 1991). Mixed with aqueous ferrous ions, hydrogen peroxide could generate hydroxyl radicals from Fenton system (Scialdone *et al.*, 2013). Hydrogen peroxide generation from dissolved oxygen was studied in acidic solutions (pH = 2). Significant self-decomposition of H<sub>2</sub>O<sub>2</sub> was observed at high pH (>9) and high temperature (>23 °C) (Z. Qiang *et al.*, 2002).

The great interest for these indirect electrooxidation methods arises from the fact that reactions involved in the cathodic reduction of oxygen proceed at low potential and in homogeneous environment (Kornienko & Kolyagin, 2003). H<sub>2</sub>O<sub>2</sub> electrosynthesis can be performed with divided or undivided cells, which show very different behavior depending on the cathode and operational parameters.

### **2.3.1 Cathode materials**

Various materials were used as cathode to generate hydrogen peroxide, such as titanium, graphene, mercury, carbon cloth, and three-dimensional electrodes, carbon felt, activated carbon fiber, reticulated vitreous carbon. They showed different features under specific conditions. Cathode material influences the contacting surface area, conductivity, current density, chemical resistance, all of which are critical indicators to decide the generation of hydrogen peroxide.

Mercury has been disregarded for potential cathode material owing to its toxicity. Carbon, unlike mercury, has no toxicity and exhibits high over potentials for H<sub>2</sub> evolution, low catalytic activity and conductivity. Various kinds

of carbon were investigated for H<sub>2</sub>O<sub>2</sub> production. Bare graphite, activated carbon with graphite, and carbon nanotubes with graphite were investigated (Khataee *et al.*, 2011). The results showed carbon nanotubes with graphite had the best performance among them, 118.65 μM H<sub>2</sub>O<sub>2</sub> in water, nearly three times higher than activated carbon with graphite, seven times higher than bare graphite. Diamond doped with boron was used as cathode as well (Isarain-Chávez *et al.*, 2013). A concentration of 82 mg L<sup>-1</sup> H<sub>2</sub>O<sub>2</sub> was achieved with 31 mA cm<sup>-2</sup> current density. Due to the low solubility of oxygen in aqueous solution at room temperature and 1 atmospheric pressure, 44 mg L<sup>-1</sup> for saturated solubility, conversion efficiency of dissolved oxygen becomes an important factor for H<sub>2</sub>O<sub>2</sub> production. Gas diffusion electrode (GDE) contacted the solution at its carbon surface when percolation of the injected gas passed across its thin and porous structure. The large number of active surface area led to a fast reduction reaction and accumulation of H<sub>2</sub>O<sub>2</sub> (Gallegos *et al.*, 2005). Prussian Blue was used as cathode in a high performance H<sub>2</sub>O<sub>2</sub> fuel cell, silver and nickel as anode materials in an acidic medium was realized by Shaegh *et al.* (Shaegh *et al.*, 2012).

Although quite a lot materials were used as cathode to produce hydrogen peroxide, few studies mentioned carbon nanotubes treated with nitric acid or hydrogen chloride acid as cathode for H<sub>2</sub>O<sub>2</sub> production, and few of them were tested for their long-term stability and reliability. In this study, carbon nanotubes dealt with certain treatments, calcination, acid treatments were compared on their H<sub>2</sub>O<sub>2</sub> production performance.

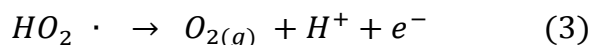
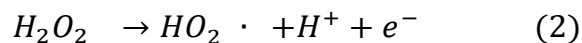


### 2.3.2 Divided reactors

Some reactors were divided for anolyte and catholyte separately for different solutions. The high current efficiency for H<sub>2</sub>O<sub>2</sub> production was approximately 85%, with H<sub>2</sub>O<sub>2</sub> accumulation in 0.5 M Na<sub>2</sub>SO<sub>4</sub> at – 0.6 V vs Ag/AgCl/KCl cathode potential (Sudoh *et al.*, 1986). Higher current efficiency around 92% was achieved by Do and Chen (2007). A gas diffusion electrode system in divided reactor was reported excellent performance, 98 – 100% current efficiencies for hydrogen peroxide recirculating 0.05 M Na<sub>2</sub>SO<sub>4</sub> with carbon-PTFE in a two-electrode divided system (Agladze *et al.*, 2007). On the contrary, Panizza and Cerisola (2008) only gained a low efficiency, 47%, with a three-electrode cell and an O<sub>2</sub>-diffusion cathode.

### 2.3.3 Undivided reactors

The advantage of undivided reactor for electrochemical reaction is the lower potential or voltage it needed for electrolysis because the potential or voltage did not avoided between anode and cathode. However undivided reactor led to a more complicated environment for hydrogen peroxide, some reactive oxygen species and weaker oxidants might be produced in it. When an undivided cell is utilized, H<sub>2</sub>O<sub>2</sub> is also oxidized to O<sub>2</sub> at the anode via HO<sub>2</sub>• as an intermediate by reactions 2 and 3:



Brillas (2000) investigated H<sub>2</sub>O<sub>2</sub> accumulation with two electrodes in a statistic undivided cell first. The H<sub>2</sub>O<sub>2</sub> concentration showed linearly

relationship with applied current. From his results, the higher current applied the higher concentration of H<sub>2</sub>O<sub>2</sub> accumulated in the reactor. The highest accumulated concentration of H<sub>2</sub>O<sub>2</sub> he got was around 75 mM at 450 mA after 180 minutes.

The current efficiency of undivided cells was related to pH, dissolved oxygen, electrolysis concentration of solution. High current efficiency (100%) was achieved in acid and neutral solution in 5 minutes from 5 A to 20 A under 40 Celsius degrees (Agladze *et al.*, 2007). The efficiency decreased with the time period, only 15% after 60 minutes. The smaller gap between anode and cathode the higher current efficiency would be achieved due to better conductivity and electrons distribution. In alkaline solution, hydrogen peroxide became unstable and decomposed to oxygen. The H<sub>2</sub>O<sub>2</sub> decomposition rate reached almost 100% at pH over 13 (Qiang *et al.*, 2002). And high temperature (> 23 °C) would stimulate the decomposition as well. In his research, the optimal conditions were -0.5 V (vs. Standard Calomel Electrode),  $8.2 \times 10^{-2}$  mol oxygen per minute. 80% – 90% current efficiency was achieved and the 80 mg/L H<sub>2</sub>O<sub>2</sub> was accumulated in 120 minutes in reactor.

CNT were regarded as a new generation of oxygen reduction reaction catalyst.(Li *et al.*, 2011; Zhang *et al.*, 2004; Zhang *et al.*, 2008) In this work, the *in-situ* production of H<sub>2</sub>O<sub>2</sub> as a function of applied cathode potential, dissolved oxygen (DO), pH, cathode materials, flow rate, organic category and concentrations were systematically studied within the flow-through electrochemical CNT filter system in an undivided reactor. To the best of our

knowledge, the *in-situ* generation of H<sub>2</sub>O<sub>2</sub> production within the electrochemical CNT filter system has not been reported previously.

## **2.4 Phenol removal and oxidation**

Phenol was selected as a model aromatic compound to evaluate the system performance and its oxidation rate not only because it is toxic and refractory to conventional biological wastewater treatment (Olaniran & Igbinsa, 2011), but also because it is frequently detected in industrial and municipal sewage and has been classified by Agency for Toxic Substances & Disease Registry, USA, as the top 179<sup>th</sup> priority hazardous substances that need urgent treatment before entering into the environment ("The ATSDR 2011 Substance Priority List," 2011).

### **2.4.1 Removal methods for phenol**

Different approaches including chemical oxidation, catalytic oxidation, biodegradation, adsorption and many other technologies are used to remove phenol from aqueous solutions. It was degraded with a Fe/Cu-catalytic heterogeneous Fenton process (Yang *et al.*, 2013), with which the removal efficiency of phenol reached over 97% even after three cycles, and 53% for TOC. Biodegradation methods for phenol was conducted with native microorganism isolated from coke processing wastewater. The biodegradation of phenol was significantly affected by pH, temperature of incubation and concentration of glucose (Chakraborty *et al.*, 2010). Powdered activated carbon (PAC) was utilized on phenol for its adsorption performance (Chakraborty *et al.*, 2010). Over 80% phenol was adsorbed rapidly by PAC within the initial 10 min.

## 2.4.2 Oxidation products of phenol

The catalytic oxidation of phenol has attracted considerable attention in recent years due to the important use of products generated from this reaction, namely, catechol and hydroquinone.

Phenol would be degraded to hydroquinone, *p*-benzenequinone and catechol after oxidation reaction (Yang *et al.*, 2013). The main mechanism of phenol oxidation might be the thatortho- and para-substitution reaction by hydroxyl. This catalytic oxidation path of phenol is consistent with Qiao (2012). All the oxidation products would be degraded into organic carboxylic acid.

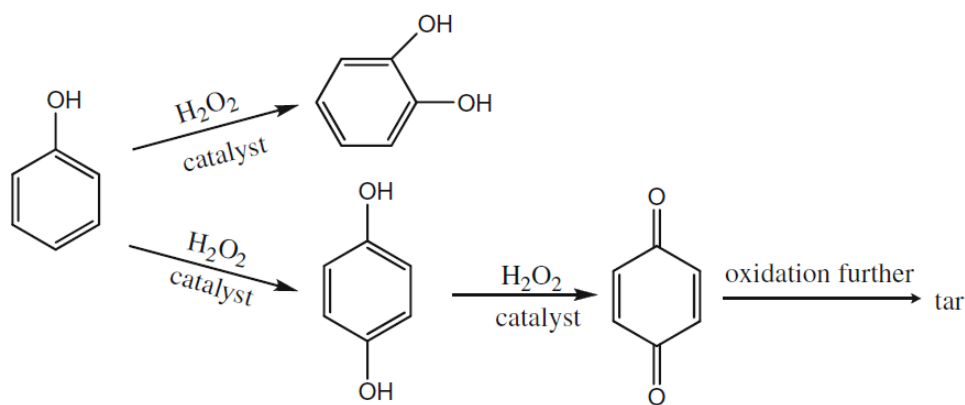


**Figure 2-1. Catalytic oxidation reaction of phenol**

From reference: Determination of catalytic oxidation products of phenol by RP-HPLC(Qiao *et al.*, 2012)

## 3 MATERIALS AND METHODS

### 3.1 Chemicals and materials

Sodium sulphate ( $\text{Na}_2\text{SO}_4$ ,  $\geq 99.0\%$ ), hydrochloric acid (HCl, ACS reagent, 37%), potassium iodide (KI, ACS reagent,  $\geq 99.0\%$ ), ammonium molybdate ( $(\text{NH}_4)_2\text{MoO}_4$ , 99.98% trace metals basis), potassium hydrogen phthalate ( $\text{C}_8\text{H}_5\text{KO}_4$ , BioXtra,  $\geq 99.95\%$ ), sodium hydroxide (NaOH, ACS reagent,  $\geq 97.0\%$ ), were purchased from Sigma-Aldrich (St. Louis, MO). Ethanol (EtOH) and n-methyl-2-pyrrolidone (NMP, ACS grade,  $> 99.0\%$ ) were purchased from VWR (Singapore). Aqueous solutions were prepared with deionized water (DI- $\text{H}_2\text{O}$ ) from an ELGA PURELAB Option system (Singapore) with a resistivity of  $\geq 18.2 \text{ M}\Omega\cdot\text{cm}^{-1}$ . Multi-walled carbon nanotubes (CNT) were purchased from NanoTechLabs (Yadkinville, NC).

### 3.2 Electrochemical carbon nanotubes filter preparation

Three types of CNT with the same length ( $\langle l \rangle = 100 \mu\text{m}$ , provided by the manufacturer) were used: C-grade ( $\langle d \rangle = 15 \text{ nm}$ , BET =  $88.5 \text{ m}^2/\text{g}$ ), M-grade ( $\langle d \rangle = 40 \text{ nm}$ , BET =  $34.6 \text{ m}^2/\text{g}$ ), and J-grade ( $\langle d \rangle = 100 \text{ nm}$ , BET =  $30.3 \text{ m}^2/\text{g}$ ).

The cathodic and anodic filters were produced by dispersing 15 mg CNT into NMP at  $0.5 \text{ mg mL}^{-1}$  and probe sonication for 15 min. The post-sonicated homogeneous dispersion of CNT and NMP were then vacuum-filtered onto a  $5 \mu\text{m}$  Millipore JMWP PTFE membrane (Billerica, MA) and washed sequentially by 100 mL ethanol, 100 mL of 1:1 DI- $\text{H}_2\text{O}$ :ethanol and 250 mL DI- $\text{H}_2\text{O}$  before

use. 10 mmol L<sup>-1</sup> of Na<sub>2</sub>SO<sub>4</sub> was used as a background electrolyte to normalize ionic strength and conductivity.

### **3.3 Carbon nanotube surface treatment**

To study the effect of different CNT surface chemistry on H<sub>2</sub>O<sub>2</sub> production, various conventional treatment technologies were applied to generate a set of multi-walled CNT, including raw CNT (without any post-treatment), C-CNT (raw CNT calcinated at 350 °C for 1 h to remove amorphous carbon within the nanotubes), C-CNT-HCl (calcinated at 350 °C for 1 h and further refluxed in HCl at 70 °C for 12 h to remove the remaining iron/iron oxide catalyst), C-CNT-HNO<sub>3</sub> (calcinated at 350 °C for 1 h and refluxed in HNO<sub>3</sub> at 70 °C for 12 h). After acid reflux treatment, CNT was filtrated through 5 μm PTFE membrane, and then dried in oven at 60 °C for 12 h.

### **3.4 Electrochemical filtration apparatus and characterization**

All filtration experiments were conducted with an electrochemically modified Whatman filtration casing (Piscataway, NJ) as described in a previous study (Schnoor & Vecitis, 2013). Briefly, two PTFE-supported CNT network served as the cathode and anode, respectively, as shown in figure 3-1. Two PTFE-supported CNT network served as the cathode and anode. Both CNT networks were mechanically contacted with a titanium current collector and the electrochemistry was driven by a CH Instruments Electrochemical Analyzer (CHI604E) (Austin, TX) with Ag/AgCl reference electrode for experiments. Additionally, a titanium cathode was also utilized to compare the effect of

cathode materials on both H<sub>2</sub>O<sub>2</sub> production and phenol oxidation. After sealing the filtration casing and priming with DI-H<sub>2</sub>O, a Masterflex L/S digital peristaltic pump (Singapore) was used to flow DI-H<sub>2</sub>O through the filter to rinse and calibrate. Then the phenol solution containing different DO was pumped into the filter and effluent aliquots of phenol was collected and quantified by its absorption at 270 nm ( $\epsilon = 1310 \text{ M}^{-1} \text{ cm}^{-1}$ ) with a Shimadzu UV-1800 spectrophotometer (Singapore). Total organic carbon (TOC) of phenol samples were measured using a Shimadzu TOC-V<sub>CPH</sub> total organic carbon analyzer (Singapore) with phosphoric acid oxidation. Five standard solutions were made from potassium hydrogen phthalate (for total carbon calibration) and sodium carbonate (for total inorganic carbon calibration), respectively, over the range 0-100 mg C L<sup>-1</sup> and used to calibrate the TOC. The electrochemical filtration system was operated at a flow rate of 1.5 mL min<sup>-1</sup> unless otherwise noted and a 10 mmol L<sup>-1</sup> of Na<sub>2</sub>SO<sub>4</sub> was used as a background electrolyte to normalize ionic strength and conductivity. The chronoamperometry and cyclic voltammograms measurements were completed with the CHI604E electrochemical analyzer using a three-electrode system: a cathodic CNT working electrode, an Ag/AgCl reference electrode, and an anodic CNT electrode.

### **3.5 Characterization of carbon nanotubes filters**

Field emission scanning electron microscopy (FESEM) was conducted on a Zeiss FESEM Supra55VP and *ImageJ* (NIH) software was used to analyse the obtained electron micrographs.

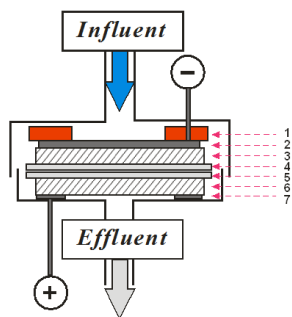


**Figure 3-1. Schematic diagram of electrochemical reactor**  
 1-rubber ring; 2-titanium plate; 3,6-CNT membranes;  
 4,5-PTFE membranes; 7-titanium ring

### 3.6 pH and dissolved oxygen analysis

Concentrations of pH and dissolved oxygen of the influent and effluent were measured using an Agilent 3200M multi-parameter analyzer (Singapore) and a P3211 probe and a D6111 probe, respectively. pH was tuned with, respectively, 1 mol L<sup>-1</sup> hydrochloric acid and sodium hydroxide solution. O<sub>2</sub> was injected into the solution before the experiment by an O<sub>2</sub> cylinder and N<sub>2</sub> was injected to provide a deoxygenated condition.

### 3.7 Hydrogen peroxide determination method

The H<sub>2</sub>O<sub>2</sub> production experiments were conducted via pumping the Na<sub>2</sub>SO<sub>4</sub> solution alone throughout the electrochemical filter. The concentration of hydrogen peroxide was measured by the potassium iodide method.(Beckett & Hua, 2001; Kormann, 1988). The iodide ion (I<sup>-</sup>) will rapidly react with H<sub>2</sub>O<sub>2</sub> to form the triiodide ion (I<sup>3-</sup>) that presents strong absorption at wavelength of 352 nm ( $\epsilon=26\ 000\ \text{M}^{-1}\text{cm}^{-1}$ ). The 0.2 mL sample aliquots from each experiment were mixed in a quartz cuvette containing 1.0 mL of 0.10 mol L<sup>-1</sup> potassium biphthalate and 0.75 mL of solution containing 0.4 mol L<sup>-1</sup> potassium iodide,



0.06 mol L<sup>-1</sup> sodium hydroxide, and 10<sup>-4</sup> mol L<sup>-1</sup> ammonium molybdate. The mixed solutions (total volume of 1.95 mL) were allowed to stand for 2 min to stabilize before the absorbance measurement. All absorbance values were measured at ambient temperature using a Shimadzu UV-1800 spectrophotometer (Singapore).

### 3.8 Phenol, Methyl orange, tetracycline, geosmin and MIB determination method

Aqueous phenol concentration in effluent water was determined by spectrophotometer at 352 nm. A calibration curve converting absorption to concentration is shown in Figure 3-2. Effluent aliquots of methyl orange and tetracycline were collected and quantified at 462 nm and 355 nm ( $\epsilon = 13320 \text{ M}^{-1} \text{ cm}^{-1}$ ) with a spectrophotometer (Shimadzu, UV-1800). Effluent geosmin and MIB were determined by GC-MS.

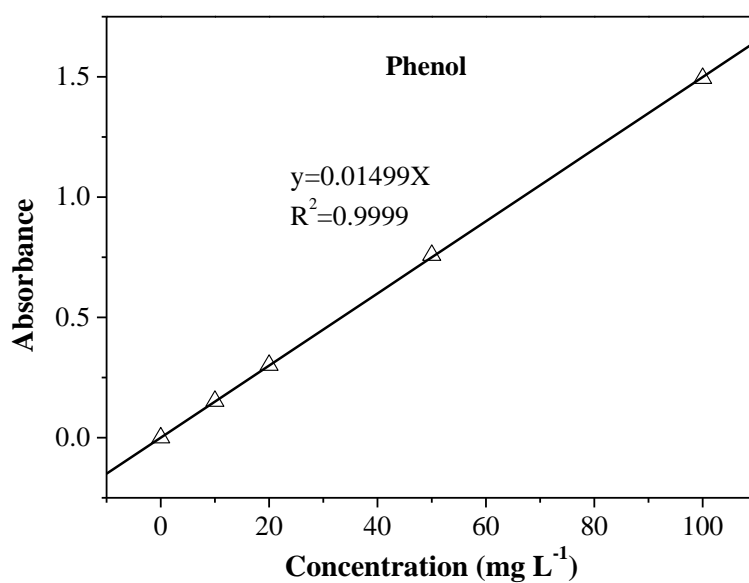


**Figure 3-2. Calibration curve of phenol.**

## **4 HYDROGEN PEROXIDE PRODUCTION WITH ELECTROCHEMICAL CARBON NANOTUBES SYSTEM**

The performance of electrochemical CNT filters in the degradation of organic pollutants are related to the amount of H<sub>2</sub>O<sub>2</sub> and/or other reactive oxygen species produced in the medium, which are affected by the cathode materials, applied potential, flow rate, pH, and DO concentrations. (Pignatello, Oliveros, & MacKay, 2006b) In this study, the influences of these factors to H<sub>2</sub>O<sub>2</sub> production and relevant electrochemical characteristics were investigated.

### **4.1 Cyclic voltammetry**

Cyclic voltammetry (CV) for the CNT cathodes were measured to examine the fundamental oxygen electrochemical characteristics within the electrochemical filter as shown in figure 3-1. The CV curves under saturated O<sub>2</sub> (44 mg L<sup>-1</sup>) exhibited a steep decrease in the reduction current at lower potentials, and the lower currents were observed with higher initial DO concentration, indicating excellent electro-activity of the CNT cathode for O<sub>2</sub> reduction. The reduction peak at -0.32 V (vs. Ag/AgCl) can be ascribed to the generation of hydrogen peroxide via a 2e<sup>-</sup> O<sub>2</sub> reduction process (Eq. 1). Contrarily, there was no obvious current peak under deoxygenated conditions.

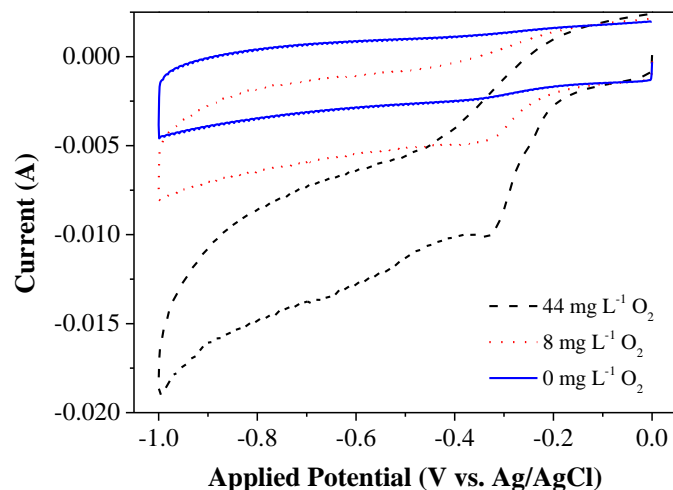


**Figure 4-1. Cyclic voltammetry curves of the CNT electrochemical filter as a functional applied cathode potential and DO levels.**

Experimental conditions:  $\text{Na}_2\text{SO}_4 = 10 \text{ mmol L}^{-1}$ , flow rate =  $1.5 \text{ mL min}^{-1}$ .

## 4.2 Comparison of electro-generation of $\text{H}_2\text{O}_2$ in solutions with different pH values

Influent pH was an important impact factor on the electroreduction of  $\text{H}_2\text{O}_2$  (Figure 4-2). In order to investigate the electro-generation of  $\text{H}_2\text{O}_2$  in acid, neutral and alkaline solutions, several experiments were performed in the undivided electrolysis system containing  $10 \text{ mM Na}_2\text{SO}_4$  at a flow rate of  $1.5 \text{ mL/min}$ .

Compared with the basic and acid conditions, the neutral pH condition presented the highest  $\text{H}_2\text{O}_2$  yield, although the improvement was not significant ( $<18\%$ ). The optimum yield of  $\text{H}_2\text{O}_2$  was obtained at  $-0.4 \text{ V}$  (vs.  $\text{Ag/AgCl}$ ) for all three pH conditions.

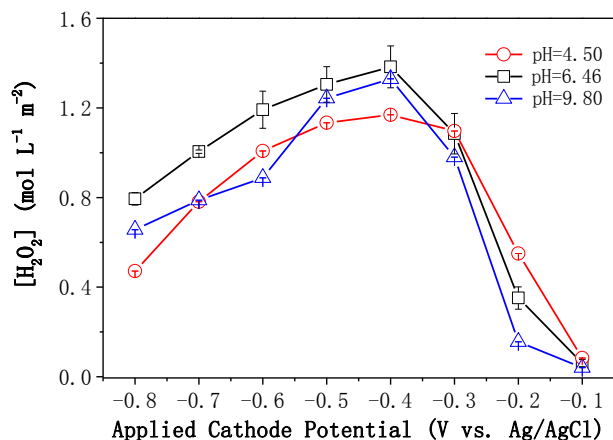


**Figure 4-2. Electrochemical H<sub>2</sub>O<sub>2</sub> yield as a function of pH**  
 Experimental conditions: Na<sub>2</sub>SO<sub>4</sub> = 10 mmol L<sup>-1</sup>, flow rate = 1.5 mL min<sup>-1</sup>

Influent solutions were adjusted to acid (pH = 4.50), neutral (pH = 6.46) and alkaline (pH = 9.80) with NaOH and H<sub>2</sub>SO<sub>4</sub>. For each solution, increasing cathode potentials were applied on reactor from -0.8 V to -0.1 V vs. Ag/AgCl reference electrode. Figure 4-2 shows the change of H<sub>2</sub>O<sub>2</sub> yield with cathode potentials in different pH solutions. In all three solutions, the H<sub>2</sub>O<sub>2</sub> yield soared from 0.4 – 0.8 mol L<sup>-1</sup> m<sup>-2</sup> to 1.1 – 1.4 mol L<sup>-1</sup> m<sup>-2</sup> with increasing cathode potential from -0.8 V to -0.4 V. The H<sub>2</sub>O<sub>2</sub> yield peaked at -0.4 V, after which it decreased gradually to less than 0.1 mol L<sup>-1</sup> m<sup>-2</sup>. The neutral one showed better performance than acid and alkaline in H<sub>2</sub>O<sub>2</sub> generation for its higher concentration (its peak concentration were 18.15% higher than that in acid) and more stable sequential generation in lower cathode potential. The one in acid showed lower H<sub>2</sub>O<sub>2</sub> concentration and instability for harsh increasing and decreasing with changes in cathode potentials. So the optimized cathode potential versus reference electrode was at -0.4 V for three different pH. Either higher or lower potential decreased the production of H<sub>2</sub>O<sub>2</sub>, especially for two in acid and alkaline.

### **4.3 Comparison of electro-generation of H<sub>2</sub>O<sub>2</sub> with different dissolved oxygen**

Oxygen gas was first dissolved in the aqueous phase and further transferred from the bulk liquid to the cathodic surface, where it was reduced to hydrogen peroxide. As one reactant of H<sub>2</sub>O<sub>2</sub>, dissolved oxygen in solution could restrict the production of H<sub>2</sub>O<sub>2</sub> as well. To quantify the amount of H<sub>2</sub>O<sub>2</sub> generated from influent with different dissolved oxygen concentration, data was collected from experiments and plotted in figure 4-3. The concentration of DO was controlled through aeration with oxygen or nitrogen which could eliminate oxygen in solution.

Since O<sub>2</sub> was the main reactant to produce H<sub>2</sub>O<sub>2</sub>, H<sub>2</sub>O<sub>2</sub> yield increased with higher initial DO concentrations. The maximum H<sub>2</sub>O<sub>2</sub> yield was obtained at an applied cathode potential of -0.4 V (vs. Ag/AgCl) at saturated DO concentration of 44 mg L<sup>-1</sup>, which was 1.7-, 2.8- and 46.8-fold higher than those at DO concentrations of 30, 15, and 0 mg L<sup>-1</sup>, respectively. The production was in positive correlation with dissolved oxygen. The higher the dissolved concentration was, the greater amount of H<sub>2</sub>O<sub>2</sub> in effluent was gained. For solutions with dissolved oxygen concentration of 15, 30 mg/L, both of them had similar H<sub>2</sub>O<sub>2</sub> generation trends with that of 44 mg/L DO concentration. The optimized cathode potential for production was -0.4 V for all three DO values. When cathode potential was applied over -0.3 V on the one with 15 mg/L DO, the H<sub>2</sub>O<sub>2</sub> concentration met its ceiling, 11.4 mg/L in effluent on average (10.8 – 11.8 mg/L). The corresponding dissolved oxygen efficiency was 69.1% (66.2% - 71.9%). While the upper limit of H<sub>2</sub>O<sub>2</sub> concentration in 30 mg/L DO solution was above -0.4 V. 15.7 mg/L H<sub>2</sub>O<sub>2</sub> were measured on average in effluent (14.5 – 16.6 mg/L) from -0.4 V to -0.7 V.

Its average DO efficiency was 49.3% (45.6% - 52.2%), much lower than that of 15 mg/L DO. At -0.8 V, there was a slight decline in H<sub>2</sub>O<sub>2</sub> field, indicating at high voltage the electron distribution mechanism changed, less electrons participating H<sub>2</sub>O<sub>2</sub> generation reaction. The solution with 44 mg/L oxygen, which was aeration saturated with oxygen in influent, showed H<sub>2</sub>O<sub>2</sub> concentration with over three times higher than the one with 15 mg/L DO, peaked at -0.4 V, 33.2 mg/L H<sub>2</sub>O<sub>2</sub>. The DO efficiency for oxygen saturated solution were 71.0%, even 2% higher than the 15 mg/L DO solution.

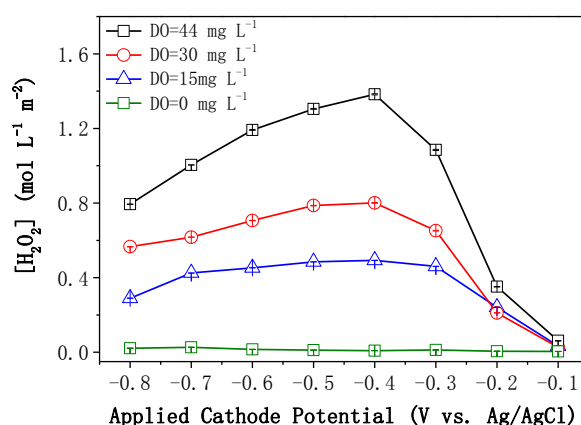


**Figure 4-3. Electrochemical H<sub>2</sub>O<sub>2</sub> yield as a function of DO**  
 Experimental conditions: Na<sub>2</sub>SO<sub>4</sub> = 10 mmol L<sup>-1</sup>, flow rate = 1.5 mL min<sup>-1</sup>

#### 4.4 Electro-generation of H<sub>2</sub>O<sub>2</sub> with different flow rate

All the data mentioned above was gained at a flow rate of 1.5 mL/min. As a critical factor influencing H<sub>2</sub>O<sub>2</sub> production and deciding wastewater treatment capacity, flow rate is plotted versus H<sub>2</sub>O<sub>2</sub> yield to quantify its effect in figure 4-4.

The effects of flow rates on electroreduction for H<sub>2</sub>O<sub>2</sub> generation was examined under optimized conditions (C-CNT-HCl, applied cathode potential = -0.4 V (vs. Ag/AgCl), DO = 44 mg L<sup>-1</sup>, pH = 6.5, and [Na<sub>2</sub>SO<sub>4</sub>] = 10 mmol L<sup>-1</sup>,

Figure 4-4), as flow rate was an important parameter influencing the kinetics within electrochemical systems (Schnoor & Vecitis, 2013; Vahid & Khataee, 2013). At low flow rates below  $1.5 \text{ mL min}^{-1}$ ,  $\text{H}_2\text{O}_2$  yield increased linearly with increased flow rates, from  $11.0 \text{ mg/L}$  to  $26.9 \text{ mg/L}$ , indicating that the filtration system was under mixed mass transfer and oxygen reduction reaction control. At medium flow rate conditions ( $1.5\text{-}4.0 \text{ mL min}^{-1}$ ), the system became mass-transfer-limited,  $\text{H}_2\text{O}_2$  production maintained around  $28.6 \text{ mg/L}$  with slight fluctuation, i.e., the electroreduction rate of  $\text{O}_2$  was limited by the flow rate of the influent  $\text{Na}_2\text{SO}_4$  solution throughout the cathode and subsequent replenishment of  $\text{O}_2$  to produce  $\text{H}_2\text{O}_2$ . High flow rates above  $4 \text{ mL min}^{-1}$  may be detrimental to the reduction kinetics due to greatly increased pressure within the current filtration casing,  $25.1 \text{ mg/L}$  for  $\text{H}_2\text{O}_2$  production, which may directly destroy the thin CNT membrane (Schnoor & Vecitis, 2013). This is in consistent with the results obtained by Qiang and co-workers, which indicate that further increase in flow rate after the optimal value may not improve the  $\text{H}_2\text{O}_2$  production (Qiang *et al.*, 2002).

The average current efficiency for ascending period was 66.3% (minimum: 57.2%, maximum: 83.8%), over 30% higher than that for the stable period (average: 35.2%, 27.4% – 48.3%). After flow rate reached  $1.5 \text{ mL/min}$ , the electrons distribution at such conditions had been maximized for reduction reaction, and the DO efficiency as well (61.7% for stable period). The  $\text{H}_2\text{O}_2$  concentration and relevant chemical characteristics over  $5.0 \text{ mL/min}$  flow rate did not been measured in this study.

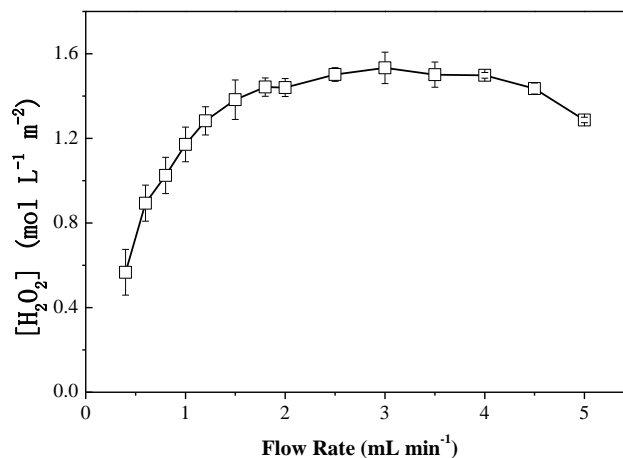


**Figure 4-4. Electrochemical H<sub>2</sub>O<sub>2</sub> yield as a function of flow rate**

#### **4.5 Electro-generation of H<sub>2</sub>O<sub>2</sub> with different grade CNT membranes**

Since the properties of functional materials are highly dependent on their microstructures, H<sub>2</sub>O<sub>2</sub> yield were affected by the functional CNT cathodes with different dimensions (Figure 4-5).

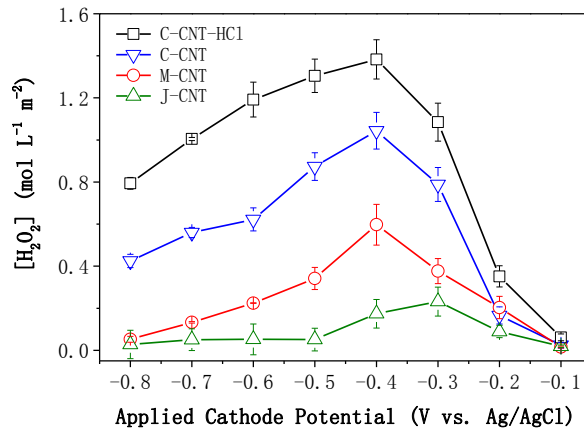
Three different dimensions of CNT were investigated for its effect on H<sub>2</sub>O<sub>2</sub> field. C-grade CNT has the biggest BET as shown in Table 4-1, 88.50 m<sup>2</sup>/g, because of the smallest diameter among three grades CNT (15 nm). BET explains the physical adsorption of gas molecules on a solid surface and serves as the basis for an important analysis technique for the measurement of the specific surface area of a material. The BET of J grade CNT is only 30.29 m<sup>2</sup>/g, and its diameter is 100 nm. The length of all three grades CNT is 100 μm. The bigger BET surface area the CNT has, the more contact area it has for solution to react, which will lead to higher efficiency in theory.



**Table 4-1. Dimension and BET for different grade carbon nanotubes**

	Dimension	BET (m <sup>2</sup> /g)
C-Grade CNT	<d> = 15 nm <l> = 100 μm	88.50
M-Grade CNT	<d> = 40 nm <l> = 100 μm	34.57
J-Grade CNT	<d> = 100 nm <l> = 100 μm	30.29

The results of H<sub>2</sub>O<sub>2</sub> yield demonstrated that all CNT cathodes presented similar trends and the maximum yield were observed at -0.4 V (vs. Ag/AgCl), which were consistent with previous results in a batch system (Do & Chen, 1993; G. V. Kornienko, Chaenko, eva, & Kornienko, 2004), which showed that H<sub>2</sub>O<sub>2</sub> yield and current efficiency gradually dropped with the applied cathode potentials decreasing toward more negative values because of side reactions, such as H<sub>2</sub> evolution from direct proton reduction (Eq. 4) and H<sub>2</sub>O<sub>2</sub> decomposition reaction (Eq. 5).

**Figure 4-5. Electrochemical H<sub>2</sub>O<sub>2</sub> yield as a function of CNT dimensions**

Experimental conditions: Na<sub>2</sub>SO<sub>4</sub> = 10 mmol L<sup>-1</sup>, flow rate = 1.5 mL min<sup>-1</sup>

The field from three grades CNT membranes showed the same order as their BET area. C grade CNT with highest physical adsorption surface area had the best

performance at same condition. It ascended to climax, 25 mg/L at optimized potential and conditions (-0.4 V cathode potential, 1.5 mL/min flow rate, 10 mM Na<sub>2</sub>SO<sub>4</sub>), and then gradually decreased to 10.2 mg/L at -0.8 V cathode potential. For M grade, it had a similar trend with C grade, yet the hydrogen peroxide concentration was lower than that of C grade, while higher than the J grade. Its maximum concentration was 14.3 mg/L, 57% of the one from C grade. And its climax was also at -0.4 V cathode potential. J grade membrane showed the lowest hydrogen peroxide concentrations among three grades because of its smallest BET area. It increased from 0.5 mg/L H<sub>2</sub>O<sub>2</sub> production at -0.1 V cathode potential to 5.6 mg/L, then it dropped to 0.6 mg/L, close to initial production at low cathode potential. All three grade CNT had low H<sub>2</sub>O<sub>2</sub> production at low cathode potential, especially for -0.1 V, only 0.5 mg/L H<sub>2</sub>O<sub>2</sub> was generated. The H<sub>2</sub>O<sub>2</sub> production showed positive relations with the dimension and BET area of CNT particles. The smaller dimension (smaller diameter) it has, the higher H<sub>2</sub>O<sub>2</sub> production it shows because the surface area per gram for reaction increases when it has smaller diameter. So the H<sub>2</sub>O<sub>2</sub> generation could be improved through treatment that will enhance its surface area for reaction.

#### **4.6 Electro-generation of H<sub>2</sub>O<sub>2</sub> with different treatment process**

Different treatments, including calcination, acid treatment (hydrochloric acid, nitric acid) would influent CNT's performance on H<sub>2</sub>O<sub>2</sub> production. Calcination on carbon nanotubes was applied at 350 °C holding for 1 hour in a tube furnace for thermal treatment then cooled down to room temperature. Thermal treatment could remove amorphous or other non-CNT carbon impurities (Gao & Vecitis, 2012). These amorphous carbons may have been blocking solution entering the ends of the carbon

nanotubes, which decrease the surface area for reaction. 2.4% of amorphous carbons were measured in multiwall carbon nanotubes (Gao & Vecitis, 2011). Two types of acid treatment were completed depending on different goals, hydrochloric acid treatment and nitric acid treatment. Both treatments were completed as follows: CNT was placed into acid at the ratio of 0.5 g/mL and reflux in acid solution at 70 °C in a round-bottom flask with stirring and a condenser for 12 h. After heating, the sample was cooled to room temperature and vacuum-filtered through a 5 µm PTFE membrane (Millipore) to collect the CNT. The CNT were then washed with Milli-Q deionized water (DI) until the filter effluent pH was near DI's pH. The sample was then oven-dried at 100 °C before use. Hydrochloric acid may remove any residual metal catalyst impurities that would lead to other catalytic reaction and negative effects on results. Nitric acid treatment was completed when the oxidative formation of surface carbonyl, hydroxyl, and carboxyl groups was needed. The CNT-HNO<sub>3</sub> and C-CNT-HNO<sub>3</sub> lost more mass than CNT treated with hydrochloric acid due to oxidative formation of easily combusted surface oxy-groups (Gao & Vecitis, 2011).

In order to investigate the effects of different treatments, their H<sub>2</sub>O<sub>2</sub> fields were shown in figure 4-6. Their increasing orders in yield performance versus cathode potential was CNT ≈ C-CNT < C-CNT-HNO<sub>3</sub> < C-CNT-HCL. Similar trend of H<sub>2</sub>O<sub>2</sub> generation was observed in CNT with three different treatments. C-CNT-HCl produced 19.1 mg/L H<sub>2</sub>O<sub>2</sub> at -0.8 V while both C-CNT and raw CNT generated 9.0 mg/L H<sub>2</sub>O<sub>2</sub>, less than one half of C-CNT-HCl. The one treated with calcination and hydrochloric acid performed best because amorphous carbon blocking ends of CNT tubes and iron catalyst particles were

all removed in preparation treatments. Increasing valid surface area made higher hydrogen peroxide production possible. Its best performance was 33.2 mg/L at -0.4 V cathode potential. For cathode potential between -0.4 V and -0.1 V, the production climaxed at -0.4 V and descended quickly. At -0.1 V cathode potential, all of them showed low H<sub>2</sub>O<sub>2</sub> production, around 1.0 – 1.1 mg/L, because electrode potential didn't meet their reaction potential.

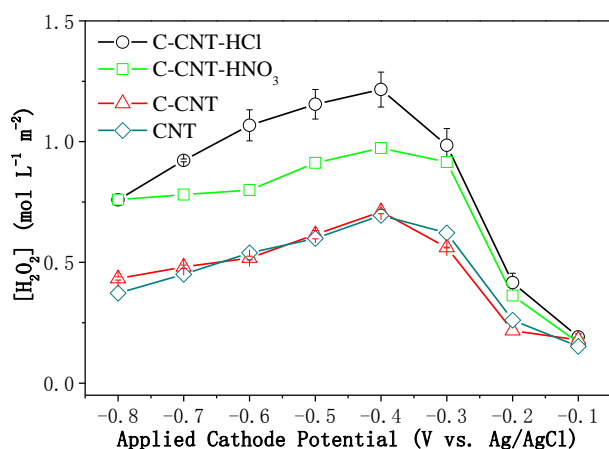


**Figure 4-6. Production of H<sub>2</sub>O<sub>2</sub> with different treatment process**

#### 4.7 Comparison of titanium and CNT cathodes

Additionally, the comparison of titanium cathode and CNT cathodes showed that H<sub>2</sub>O<sub>2</sub> yields and phenol oxidation rates were improved significantly with CNT cathodes (Figure 3). The increased specific surface area of the CNT cathodes improved total cell potential and the fraction of potential going towards the cathodes for O<sub>2</sub> reduction. (Zhang & Vecitis, 2014) The titanium cathode had a total surface area less than 15 cm<sup>2</sup> (current density of 0.05-0.50 mA cm<sup>-2</sup>), while the CNT cathode had a surface area around 5000 cm<sup>2</sup> (current density of 0.001-0.010 mA cm<sup>-2</sup>). The increase in cathode surface area greatly reduced resistance to electron transfer, and as a result increased current efficiency, extent

of H<sub>2</sub>O<sub>2</sub> production, and phenol oxidation. A recent study also indicated that by switching from a perforated titanium electrode to a CNT electrode the overall performance evidently improved and energy consumption decreased. (Schnoor & Vecitis, 2013)

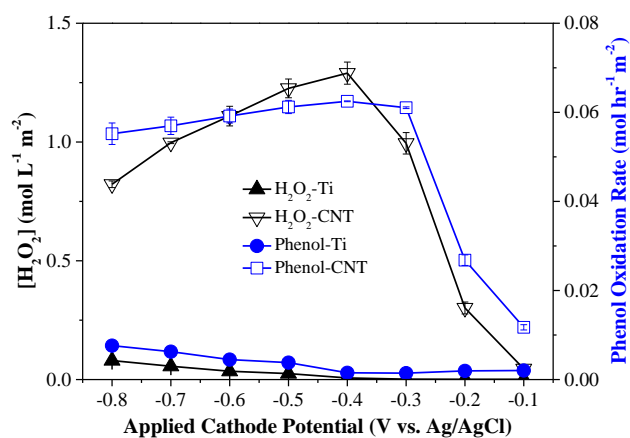


**Figure 4-7. Effect of cathode materials on H<sub>2</sub>O<sub>2</sub> yield and phenol oxidation rate: comparison of titanium cathode and CNT cathode.**

#### 4.8 Effects of cathode potential on electrochemical and effluent characteristics

Steady-state currents increased rapidly with applied cathode potentials becoming more negative till -0.4 V (vs. Ag/AgCl), from 0.15 – 0.64 mA at -0.1 V to 7.7 – 9.0 mA at -0.4 V, then increased slowly between -0.4 to -0.6 V (vs. Ag/AgCl), because of potential-independent mass transfer limit (Figure 4-8). The steady-state currents continued to increase when the applied cathode potential was below -0.6 V (vs. Ag/AgCl), 11 – 13.1 mA at -0.8 V, which suggests that other reactions, such as Eqs. 2 & 9, could have contributed to the continuously increased currents and overcome mass transfer limits. Steady-state currents were almost the same under neutral and basic pH conditions, but significantly lower under acidic conditions, which could be caused by

the higher consumption rates of electrons in the cathode (Eqs. 1 & 2). If fewer electrons were distributed to H<sub>2</sub>O<sub>2</sub> generation after -0.4 V potential, current slope would decrease little, which could explain both the decreasing H<sub>2</sub>O<sub>2</sub> production and the slope change. Current in neutral solution didn't show higher values than that in acid and alkaline ones until -0.4 V. The current in acid solution was much lower than neutral and alkaline ones, which is consistent with the production of H<sub>2</sub>O<sub>2</sub> in three pH solutions. Considering similar corresponding voltages at each cathode potential in acid and neutral solutions, the differences in current and H<sub>2</sub>O<sub>2</sub> production between acid and neutral electrolyte indicated better electron transfer ability for neutral solution. While applied cathode potential was lower than -0.4 V, alkaline electrolyte showed lower current than the other two.

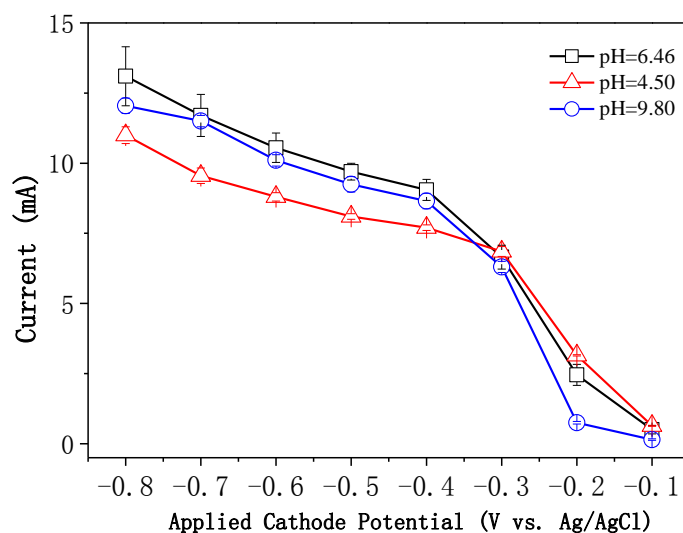


**Figure 4-8. Steady-state current as a function of applied cathode potential**

The voltage increased monotonically from 0.8 to 2.3 V with decreased applied cathode potential (Figure 4-9). Almost identical voltages were measured under neutral and acidic pH conditions, however, relatively higher voltages (>0.3-3.6%) were

obtained for basic pH when the applied cathode potentials was below -0.5 V (vs. Ag/AgCl) and relatively lower voltages (<3.7-36%) were obtained when the applied cathode potentials was higher than -0.4 V (vs. Ag/AgCl).

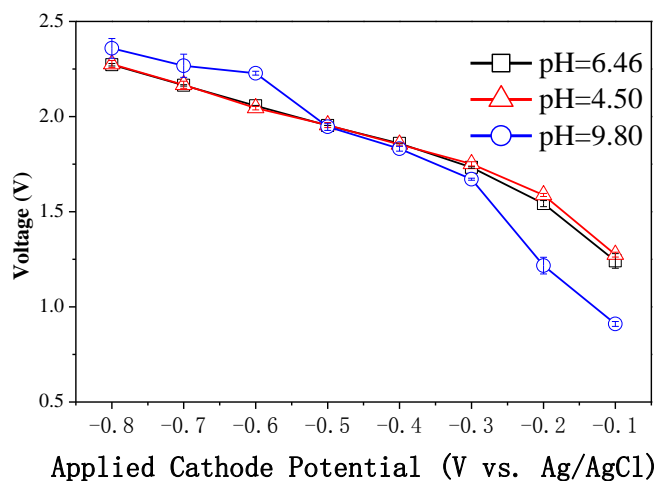
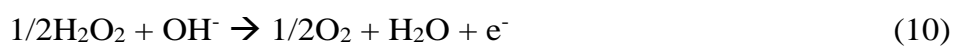


**Figure 4-9. Applied voltage as a function of applied cathode potential**

The effluent pH is a strong function of both applied cathode potential and influent pH values (Figure 4-10). Effluent pH values decreased when lower cathode potentials were applied, and effluent pH values were higher if influent pH values were higher. All three electrolytes had increasing trends in effluent pH from 5.5 – 6.5 at -0.8 V to 8.3 – 8.5 at -0.1 V. Over all alkaline electrolyte showed highest effluent pH values among the three, and acid one showed the lowest, which was in accordance with their influent pH. Even for acid solution, effluent pH (pH = 8.3, 7.3) was increased over the influent pH (4.50) at cathode potential -0.1 V and -0.2 V, indicating that cathodic processes such as water reduction to hydrogen releasing hydroxide anions were controlling the pH. The voltages for alkaline effluent were below 1.5 V, which is in agreement with results of Gao (2011). As voltages increased to 1.5 V (for cathode potential -0.2 V for acid and neutral electrolyte, -0.3 V for alkaline electrolyte), the effluent pH was approximate neutral (pH = 7.09, 7.29, 7.08) indicating that the cathodic and anodic

processes neutralize each other. When voltages rose above 1.5 V, effluent pH decreased gradually indicating the anodic processes releasing hydrogen ions dominated the pH. Although effluent showed acid, the effluent pH of alkaline one only dropped to 6.51 while the one of acid and neutral decreased to 5.48 and 5.54.

Upon application of -0.1 V (vs. Ag/AgCl) cathode potential, the effluent pH under neutral and acid conditions increased over their corresponding influent pH, indicating that hydrogen ions were readily participated into H<sub>2</sub>O<sub>2</sub> production and removed from the solution, and therefore pH was reduced. The effluent pH slightly decreased to 8.31 at -0.1 V (vs. Ag/AgCl) cathode potential under basic condition, indicating the electrogenerated H<sub>2</sub>O<sub>2</sub> were decomposed into O<sub>2</sub> and H<sub>2</sub>O rapidly under basic media via Eq. 10 and consumption of OH<sup>-</sup> decreased the effluent pH. The effluent pH then gradually decreased to nearly neutral (pH=6.56±0.25) at the applied cathode potential of -0.4 V (vs. Ag/AgCl) for all conditions, indicating that the cathodic and anodic processes neutralize each other. Once the applied cathode potential became more negative (< -0.4 V vs. Ag/AgCl), the effluent pH kept decreasing slightly suggesting other cathodic processes such as water reduction to hydrogen are dominant. The formation of visible bubbles within the filters further confirmed this hypothesis (Figure 4-11).





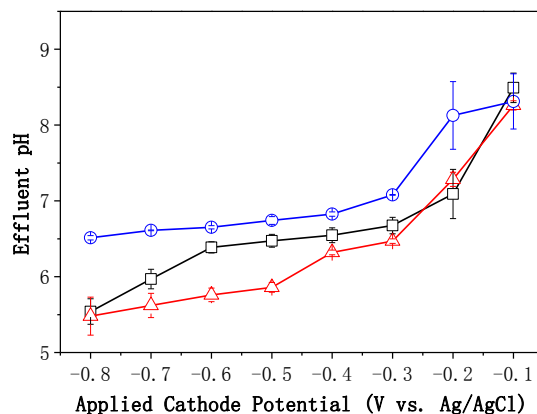


**Figure 4-10. Applied voltage as a function of applied cathode potential**

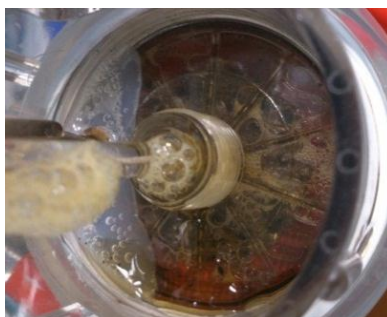
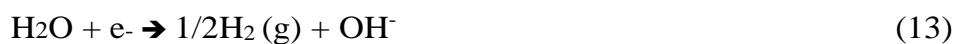


**Figure 4-11. Bubbles generated at cathode at applied cathode potential of -0.9 V (vs. Ag/AgCl).**

Cathode potential has great influences on water splitting as well. Once cathode potential was applied high enough (-0.8 V or higher, depending on different kinds of carbon nanotubes membranes), the reactor system become unstable for unexpected high voltage, soaring current, and most important, the bubbles generated at both the cathode and anode, as shown in figure 4-11. The critical point for unstable status depended on the type of carbon nanotubes membranes. For J-grade, bubbles generated when potential was over -0.4 V. With the increasing of applied cathode potential, the bubble generation rate and the bubble diameter increased quickly. The current could rise to over 80 mA, almost 8 times high than average, and large fluctuated when bubbles generated. For M-grade, the critical potential was around -0.6 V. Although bubbles

were generated at both electrodes, most amounts were observed at cathode and carried out by effluent. The composition of bubbles at cathode should be O<sub>2</sub> (Eq. 12) while those at anode should be H<sub>2</sub> (Eq. 13) with  $E^\circ = -0.83 \text{ V/SHE}$ . All the bubbles generated at voltages over 2.5 V, and the concentration of H<sub>2</sub>O<sub>2</sub> at critical point for M-grade and J-grade membranes was around 5.5 mg/L.



Effluent DO concentrations (Figure 4d) showed an inverse trend as H<sub>2</sub>O<sub>2</sub> yield (Figure 4-12) under all pH conditions, since effluent DO was remnant oxygen in solution after oxygen reduction reaction (Eq. 1). DO concentrations under acidic and basic conditions were similar and slightly lower than those under neutral pH condition. Maximum DO efficiency was achieved at an applied cathode potential of -0.4 V (vs. Ag/AgCl) (Figure 4-13). A gap was observed between the saturated influent DO (44 mg L<sup>-1</sup>) and the sum of effluent DO and the DO utilized for H<sub>2</sub>O<sub>2</sub> production. For example, a DO efficiency of 71.0% under neutral solution at -0.4 V (vs. Ag/AgCl) indicated that 71.0% of DO in the influent (31.2 mg L<sup>-1</sup>) was converted to H<sub>2</sub>O<sub>2</sub> through reduction reaction at the cathode. In addition to 7.4 mg L<sup>-1</sup> DO in the effluent, there was still a gap of 5.4 mg L<sup>-1</sup> DO disappeared in the system. The potential gas exchange between the reaction system and ambient air may release some DO and other side reactions (e.g., Eq. 10) may consume DO during the filtration process too.

The dissolved oxygen in effluent versus cathode potential in solution with different pH was plotted in figure 4-12. The effluent DO showed an exactly opposite trend of

H<sub>2</sub>O<sub>2</sub> concentration, which makes sense easily because the effluent DO is the remnant oxygen in solution after reduction reaction theoretically. Among three solutions, the neutral one had higher effluent DO, which fit its high DO efficiency. But there are gaps between saturated influent DO (44 mg/L) and DO measured in reaction system (DO consumed in H<sub>2</sub>O<sub>2</sub> generation and DO measured in effluent). H<sub>2</sub>O<sub>2</sub> could be continuously supplied from the two-electron reduction of oxygen by Eq. 1 with  $E^0 = 0.695 \text{ V/SHE}$ , which takes place more easily than its four-electron reduction to water from reaction 2 with  $E^0 = 1.23 \text{ V/SHE}$ . So the reduction of O<sub>2</sub> leads to the production of H<sub>2</sub>O instead of H<sub>2</sub>O<sub>2</sub> through the equation, resulting also in the decrease in DO efficiency and in current efficiency when the applied cathode potential was over -0.4 V. But the amount of dissolved oxygen actually participated in Eq. 9 is hard to quantify.

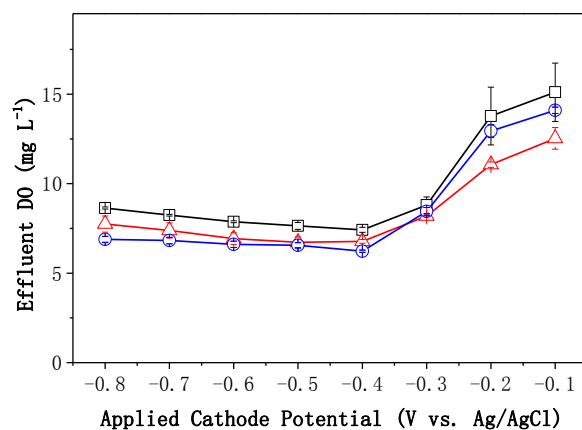


**Figure 4-12. Effluent DO concentration as a function of applied cathode potential**

Experimental conditions: Na<sub>2</sub>SO<sub>4</sub> = 10 mmol L<sup>-1</sup>, flow rate = 1.5 mL min<sup>-1</sup>

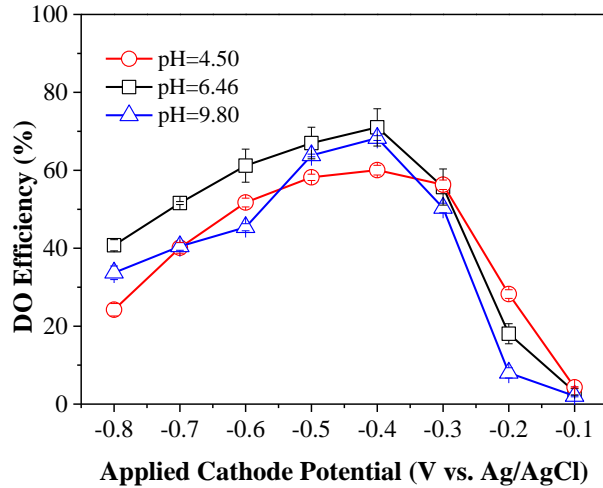


**Figure 4-13. DO efficiency as a function of pH and applied cathode potential**

As dissolved oxygen in all influents was saturated to 44 mg/L at room temperature and 1 atp, dissolved oxygen efficiency should be in well accordance with trend of H<sub>2</sub>O<sub>2</sub> field. The plot of dissolved oxygen efficiency versus cathode potential shown in figure 4-13 quantified it. DO efficiency increased gradually from 24.2% - 40.7% to peak value, 60.0% – 71.0%, and then declined to 2.1% – 4.3%. The highest DO efficiency is 71.0% for neutral solution at -0.4 V, indicating 71.0% of saturated oxygen in influent, which is 31.24 mg/L, has been converted into H<sub>2</sub>O<sub>2</sub> through reduction reaction at cathode.

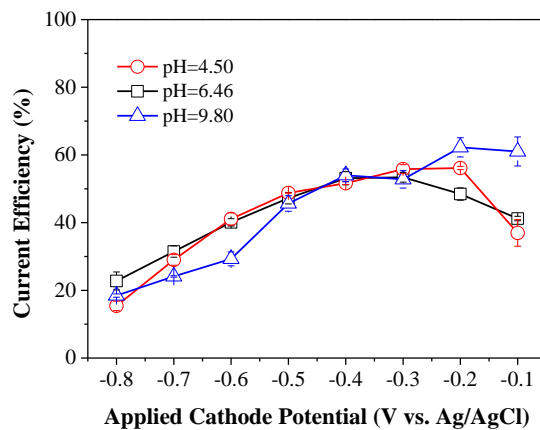


**Figure 4-14. Current Efficiency as a function of applied cathode potential**

The changes in current efficiency showed in figure 4-14 exhibits similar trends among solutions with different pH value. It indicated the proportion of electrons used in H<sub>2</sub>O<sub>2</sub> generation to all the electrons involved in the system, having no direct relationship with H<sub>2</sub>O<sub>2</sub> concentration. It increased from 15.4% – 22.8% at -0.8 V to peak and then decreased. The best current efficiency for acid, neutral and alkaline was 56.1%, 53.4% and 62.2% at -0.3 V, -0.2 V and -0.2 V, respectively. The highest efficiency was attributed to low current at low potential. The current efficiencies for best H<sub>2</sub>O<sub>2</sub> generation were 51.6%, 53.1% and 54.0% in acid, neutral and alkaline respectively, which means over half of the electrons in system contributes to H<sub>2</sub>O<sub>2</sub> generating reaction. The alkaline solution had high current efficiency at -0.1 V and -0.2 V (61.0% and 62.4%) over the other two, which is caused by exactly low current is had (0.15 mA for -0.1 V and 0.75 mA for -0.2 V), less than one-fourth of current in acid.

However, the maximum current efficiency for H<sub>2</sub>O<sub>2</sub> generation was only 52.9±1.2%, which could be explained by other H<sub>2</sub>O<sub>2</sub> decomposition processes or electron-consuming reactions. For example, H<sub>2</sub>O<sub>2</sub> could undergo chemical decomposition to O<sub>2</sub> either on the anode (heterogeneous process) or in the medium (homogeneous process, Eq. 5). Additionally, reduction from H<sub>2</sub>O<sub>2</sub> to OH<sup>-</sup> on the CNT cathodes could also consume H<sub>2</sub>O<sub>2</sub> and electron (Eq. 11). (Brillas *et al.*, 1995; Zhou *et al.*, 2008)



Other reactive species, such as OH<sup>•</sup>, may be produced by direct oxidation of hydroxyl ions (Eq. 6) and/or by electrochemical oxidation of H<sub>2</sub>O (Eq. 7). The

electrogenerated  $\text{H}_2\text{O}_2$  can also react with  $\text{OH}^\bullet$  to produce  $\text{HO}_2^\bullet$  at the anode (Eq. 8) (Haag & David, 1992) and these radicals can also be decomposed into  $\text{O}_2$  (Eq. 9). (Brillas *et al.*, 2009a; Brillas *et al.*, 1995)

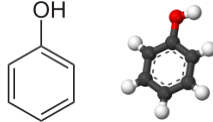


# **5 PHENOL OXIDATION BY H<sub>2</sub>O<sub>2</sub> WITH ELECTROCHEMICAL CARBON NANOTUBES FILTER**

## **5.1 Introduction of Aqueous aromatic compounds and phenol**

Aqueous aromatic compounds are toxic and refractory to conventional biological wastewater treatment. Phenol is frequently used as a model aromatic compound in industrial wastewater treatment studies as millions of tons of phenol are produced in herbicides, pharmaceutical drugs, epoxies every year as a plastics and pharmaceutical precursor (Pelegri *et al.*, 2001; Wu & Zhou, 2001). Exposure to such chemicals can damage the central nervous system, respiratory system, kidney, and blood system if entered into human body. Because of lack of treatment, unsafe transport, concentration in urban areas and inadequate management, agency for Toxic Substances & Disease Registry, USA, has classified phenols as the top 45<sup>th</sup> priority hazardous substances that need urgent treatment before entering into the environment. Therefore there is an urgent need to innovate a feasible and efficient technological process to remove aqueous phenol from waste water. Now several technologies can be performed to immediate organic compounds from water, such as bioremediation, ultraviolet radiation mineralization, advanced oxidation techniques using Fenton's reagent and so on. The limitations to these techniques are low efficiency, costly, high solvent concentrations needed to achieve good results, environmental unfriendly by products. The technology of aqueous phenol removal with on-site generating H<sub>2</sub>O<sub>2</sub> from CNT membranes could be one potential method to solve the urgent problem.

**Table 5-1. Physicochemical properties of phenol (carbolic acid)**

	Properties
Chemical name	Phenol (carbolic acid)
Molecular formula	C <sub>6</sub> H <sub>5</sub> OH
Chemical structure	
Molecular weight	94.11 g mol <sup>-1</sup>
Class	Toxic, Corrosive
Maximum absorption wavelength	352 nm

## 5.2 Statistic batch experiment for phenol removal

To evaluate whether phenol can be efficiently oxidized by H<sub>2</sub>O<sub>2</sub> alone, a 50 mg L<sup>-1</sup> phenol solution was mixed with 33 mg L<sup>-1</sup> H<sub>2</sub>O<sub>2</sub>, which contained a similar H<sub>2</sub>O<sub>2</sub> concentration to that produced by the electroreduction of O<sub>2</sub> within the electrochemical filter system. However, no significant change of phenol concentration was observed for such a solution after 2 h of mixing, indicating H<sub>2</sub>O<sub>2</sub> alone cannot oxidize phenol efficiently (Figure 5-1).

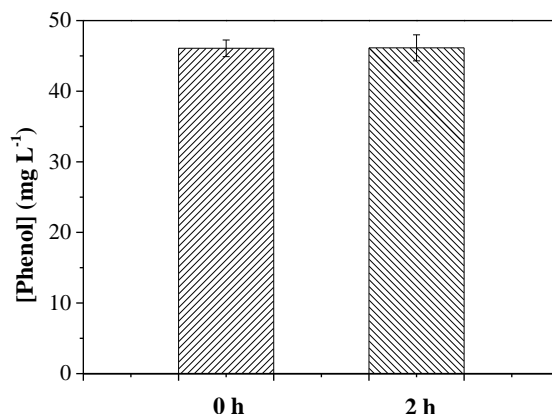


**Figure 5-1. Absorbance of 50 mg L<sup>-1</sup> phenol solution at 0 h and 2 h after adding 33 mg L<sup>-1</sup> H<sub>2</sub>O<sub>2</sub>**

Although phenol was poorly removed by H<sub>2</sub>O<sub>2</sub> at the conventional batch system, the convectively-flow system could greatly enhance mass transfer (Liu & Vecitis, 2012) and result in the high removal efficiency of phenol by H<sub>2</sub>O<sub>2</sub> oxidation in the



electrochemical CNT filter. Additionally, preliminary results here suggest that breakthrough of 50 mg L<sup>-1</sup> phenol occurred in less than 30 min by CNT sorption only (Figure 5-2), indicating the phenol molecules consumed all of the reactive surface sites and the physical adsorption to CNT filters is not sustainable for water purification.

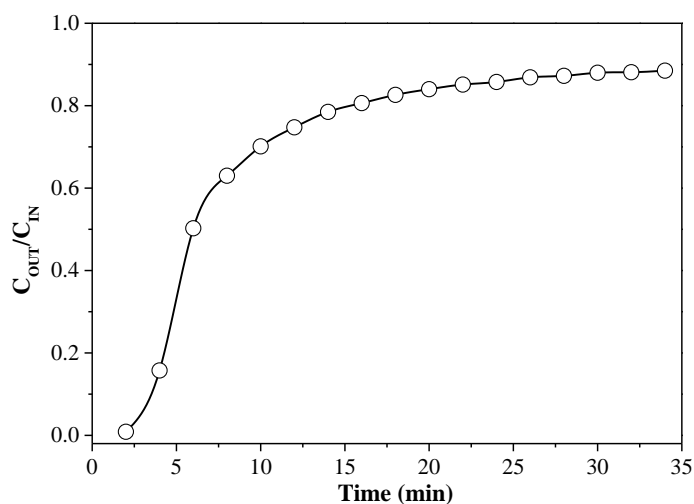


**Figure 5-2. Breakthrough curve of 50 mg L<sup>-1</sup> phenol.**

### **5.3 Phenol oxidation with different influent concentrations**

Based on previous experiments, the optimized conditions for H<sub>2</sub>O<sub>2</sub> production were applied in aqueous phenol removal experiment, applied cathode potential = -0.4 V (vs. Ag/AgCl), DO = 44 mg L<sup>-1</sup>, pH = 6.46, and flow rate = 1.5 mL min<sup>-1</sup>, electrolyte 10 mM Na<sub>2</sub>SO<sub>4</sub>.

The phenol oxidation rates under different initial phenol concentrations were shown in Figure 5-3. Three different phenol concentrations in influent, 10 mg/L, 20 mg/L, 50 mg/L, were selected to investigate its influence on effluent phenol concentration and electrochemical removal efficiency.

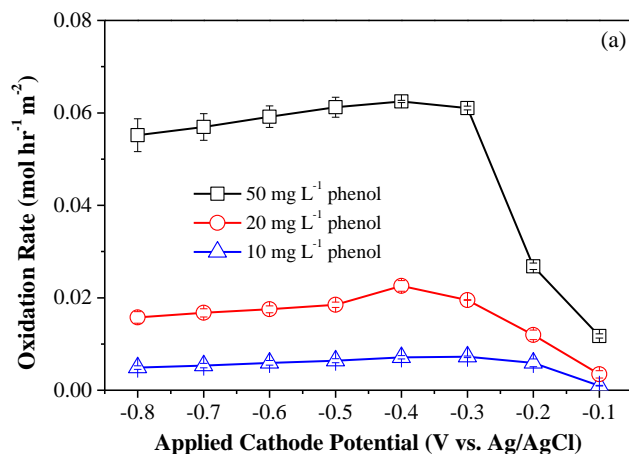


**Figure 5-3. Effect of influent phenol concentrations on phenol oxidation rate**  
 Experimental conditions: Applied cathode potential = -0.4 V vs. Ag/AgCl,  
 $[\text{Na}_2\text{SO}_4] = 10 \text{ mmol L}^{-1}$ , flow rate =  $1.5 \text{ mL min}^{-1}$ .

Maximum phenol oxidation rates were achieved at an applied cathode potential of -0.4 V (vs. Ag/AgCl), which was consistent with the  $\text{H}_2\text{O}_2$  generation rates (Figure 4-2). The maximum oxidation rates of phenol were 0.0069, 0.024 and  $0.062 \text{ mol hr}^{-1} \text{ m}^{-2}$  for 10, 20 and  $50 \text{ mg L}^{-1}$  phenol, respectively, which increased with initial phenol concentrations and can be ascribed to increased diffusion rates and enhanced mass transfer within the convectively flow system at high concentrations of phenol. The effluent concentrations of phenol decreased to 5 mg/L for 10, 20,  $50 \text{ mg L}^{-1}$  phenol at -0.4 V, respectively (Figure 5-4A). There is a floor limitation for phenol degradation using  $\text{H}_2\text{O}_2$ . Oxidation rate of phenol rose slightly from -0.8 V to -0.4 V although cathode potential, voltage and current all become lower at the best performance point. After that, oxidation rate of three solutions all decreased slightly, from  $0.06 \text{ mol hr}^{-1} \text{ m}^{-2}$ ,  $0.02 \text{ mol hr}^{-1} \text{ m}^{-2}$ ,  $0.01 \text{ mol hr}^{-1} \text{ m}^{-2}$  (removal efficiency 55.0%, 76.3% and 92.1%, Figure 5-4B) to  $0.05 \text{ mol hr}^{-1} \text{ m}^{-2}$ ,  $0.01 \text{ mol hr}^{-1} \text{ m}^{-2}$ ,  $0.005 \text{ mol hr}^{-1} \text{ m}^{-2}$  (removal efficiency 5.6%, 3.5% and 17.3%) for 10, 20,  $50 \text{ mg L}^{-1}$  phenol respectively (effluent concentration from less than 5 mg/L (4.5 mg/L, 4.7 mg/L,  $3.9 \text{ mg L}^{-1}$ ) to 9.4 mg/L, 19.3

mg/L, 41.3 mg/L at -0.1 V cathode potential). At potential of -0.1 V, minute phenol was removed from solution, which should be mostly attributed to physical absorption instead of electrochemical degradation because of its low current (at the magnitude of  $10^{-1}$  and  $10^{-2}$  mA) and electrons. Considering the fact that their  $H_2O_2$  production at best performance point should be close to each other, excess  $H_2O_2$  was generated for degrading 10 mg/L and 20 mg/L phenol in solutions, or even for the 50 mg/L one. Nonetheless effluent phenol concentration for 10 and 20 mg/L didn't show lower values than 50 mg/L. Kinetic characteristics might be one reason for their similar lowest effluent phenol concentrations. The phenol molecules and  $H_2O_2$  molecules collided with each other and reacted to degrade phenol. The collision probability fell with decreasing aqueous phenol concentration during degradation process. When aqueous phenol fell to a certain concentration, the probability for collision with  $H_2O_2$  molecules was so low that degradation reaction hardly happened during such a short time when original solution passing through the reactor. If the solution retention time in reactor was prolonged, increasing collision opportunity for degradation, phenol concentration in effluent might be shifted to an even lower level. The 50 mg/L one decreased on the smallest extent, 15.6% only, while the other two did decrease largely, 32.5% dropped for 10 mg/L influent solution, 48.8% for 20 mg/L. As they had similar lowest effluent concentrations, higher influent one showed higher removal efficiency.

The TOC removal efficiency (Figure 5-5) further demonstrated that the molecular phenol was mostly destroyed within the short residence time in the filter and oxidized into  $CO_2$ .

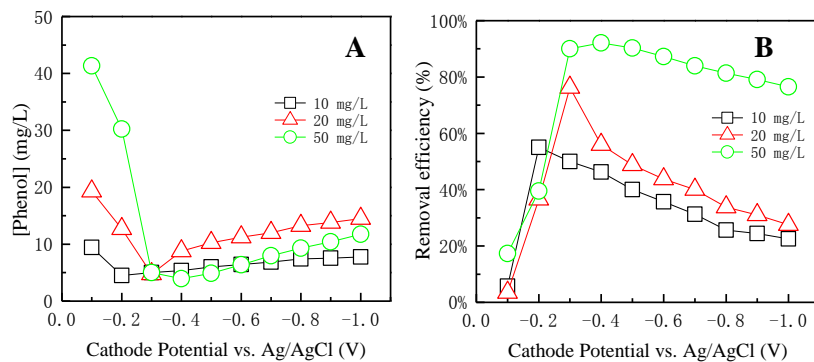


**Figure 5-4. Phenol removal experiment**  
 A. effluent [Phenol] from different influent [Phenol];  
 B. removal efficiency for different influent [Phenol]

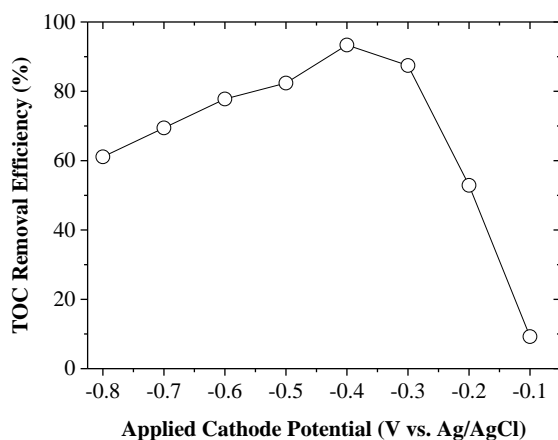


**Figure 5-5. TOC of phenol as a function of applied cathode potential.**

#### 5.4 Phenol oxidation with different DO concentrations

Additionally, phenol oxidation could be contributed by direct oxidation in the CNT anode, and therefore phenol oxidation under saturated and zero DO concentrations were compared (Figure 5-6). It can be observed from the figure that the removal effect were in accordance with DO concentration. For the solution pumped with nitrogen (almost 0 mg/L), eliminating DO basically, achieved about only 10% for removal efficiency, being likely attributed to physical absorption and electrochemical degradation. The results demonstrate that the average phenol oxidation rate sharply decreased to  $0.0082 \pm 0.0011$  mol

$\text{hr}^{-1} \text{ m}^{-2}$  when influent DO concentration was zero, which was only 13% of that obtained under saturated DO condition. Since  $\text{H}_2\text{O}_2$  production in the cathode was greatly inhibited in the deaerated solution sparged with pure  $\text{N}_2$ , the oxidation of phenol can be ascribed to the direct anodic oxidation. Those with dissolved oxygen have another mechanism to degrade phenol, generating  $\text{H}_2\text{O}_2$ , besides physical absorption and electrochemical splitting.

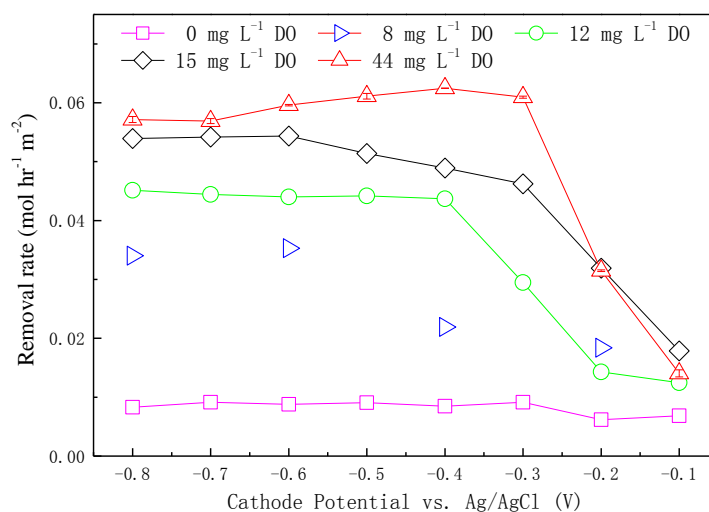


**Figure 5-6. Effect of DO on phenol oxidation rate**

Experimental conditions: Applied cathode potential =  $-0.4 \text{ V vs. Ag/AgCl}$ ,  $[\text{Na}_2\text{SO}_4] = 10 \text{ mmol L}^{-1}$ , flow rate =  $1.5 \text{ mL min}^{-1}$ .

## 5.5 Effects of different flow rate

As discussed previously,  $\text{H}_2\text{O}_2$  production is a function of flow rate. Basically high flow rate will lead to high production, which means high removal efficiency. As proof of this idea, removal efficiency and  $\text{H}_2\text{O}_2$  concentration is illustrated with different flow rate in Figure 5-7. Three stages could be concluded from the figure. From  $0.4 \text{ mL/min}$  to  $1 \text{ mL/min}$ , removal efficiency soared greatly from 67.88% to 83.50%. Above  $1 \text{ mL/min}$  to  $3.5 \text{ mL/min}$ , it ascended gently, from 83.50% to 90.25%. After the two stages, removal efficiency kept in the range of 90% to 91%. The trend of removal

efficiency fit that of H<sub>2</sub>O<sub>2</sub> production, indicating the contribution of H<sub>2</sub>O<sub>2</sub> in the degradation process of phenol.

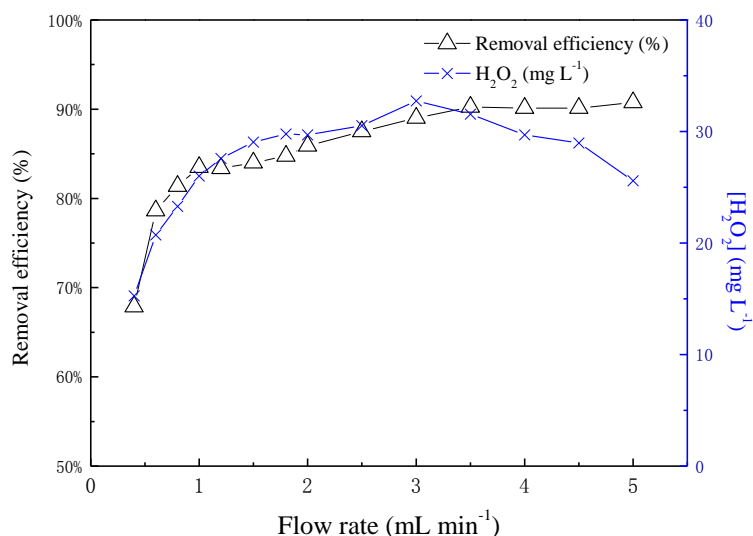


**Figure 5-7. Removal efficiency of 50 mg L<sup>-1</sup> phenol and production of H<sub>2</sub>O<sub>2</sub> with different flow rate**

## 5.6 Phenol oxidation with different grades membranes

As hydrogen peroxide production varied from different grades CNT membranes, it influenced phenol oxidation as well. Phenol removal efficiency of three grades membranes is plotted versus applied cathode potential in Figure 5-8.

Among three grades, C grade CNT membrane showed the best performance in phenol oxidation, while M grade had the lowest. The oxidation rate of three grades was in accordance with their H<sub>2</sub>O<sub>2</sub> production. The highest oxidation effect was achieved at -0.4 V cathode potential, 89%, 78% and 64% removal rate for C grade, J grade and M grade respectively. When applied cathode potential became more positive, phenol removal efficiency declined drastically, between 1% and 4% at -0.1 V potential. The high removal effect of C grade among three grades was attributed to its highest BET areas and smallest dimensions, consisting to the results in Table 4-1 and Figure 4-5.

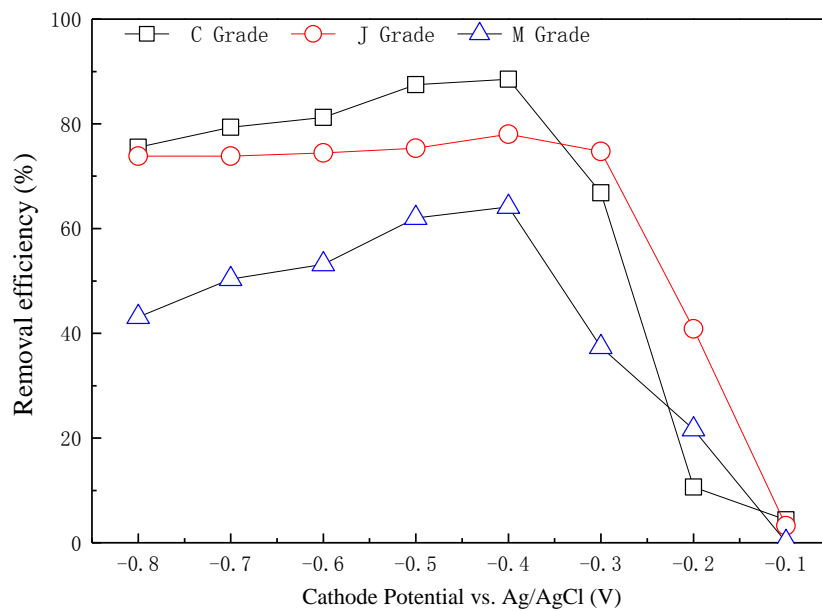


**Figure 5-8. Removal efficiency of 50 mg/L phenol with different grade CNT**

## 5.7 Effects of membranes with different treatments

Besides the factors mentioned above, different treatments, calcination, hydrogen chloride acid and nitric acid, on CNT membranes would affect the production of  $H_2O_2$  and phenol removal efficiency as well (Figure 5-9). The one treated with calcination and hydrogen chloride acid, C-CNT-HCl, performed best among three kinds of membranes, and achieved 92% for phenol removal at optimized conditions, -0.4 V cathode potential. C-CNT- $HNO_3$  and C-CNT had similar trends with C-CNT-HCl, climax at -0.4 V for 85% and 68%, respectively. Calcination could remove amorphous carbon while acid treatment could remove iron particle from CNT particles, which was the catalyst for other reactions.

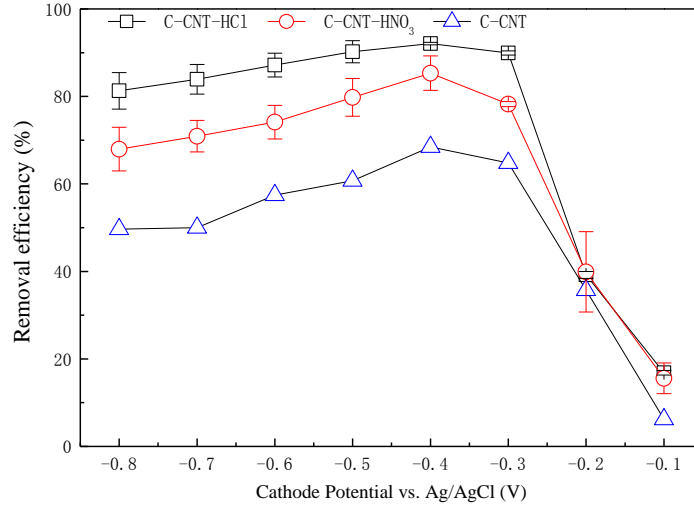


**Figure 5-9. Removal efficiency of 50 mg/L phenol with different treatment process**

## 5.8 Effects of other reactive oxygen species

In addition to electrogenerated  $\text{H}_2\text{O}_2$ , other reactive oxygen species (e.g.,  $\text{O}_2^{\bullet-}$ ,  $\text{HO}_2^{\bullet}$ ,  $\text{OH}^{\bullet}$ ) could be produced in the CNT filtration system and involved in the oxidation of phenol. Superoxide radicals,  $\text{O}_2^{\bullet-}$ , are reactive compounds produced when oxygen is reduced by electrons (Eq. 12) and occur widely in nature. (Thorpe *et al.*, 2013) These  $\text{O}_2^{\bullet-}$  are in equilibrium in aqueous solution with the hydroperoxyl radicals,  $\text{HO}_2^{\bullet}$  (Eq. 13). (Bielski, Cabelli, Arudi, & Ross, 1985) The low  $pK_a$  of  $\text{HO}_2^{\bullet}$  is only 4.8, (De Grey, 2002) which suggests that most  $\text{HO}_2^{\bullet}$  are converted to  $\text{O}_2^{\bullet-}$  under neutral condition.



To further identify the main contributors for phenol oxidation, benzoquinone ( $\text{O}_2^{\bullet-}$  scavenger, (Oshitani *et al.*, 1993; Sawada, Iyanagi, & Yamazaki, 1975)  $k = 10^9 \text{M}^{-1} \text{s}^{-1}$ ) and *tert*-butanol ( $\text{OH}^{\bullet}$  scavenger, (Buxton *et al.*,



1988; Ma *et al.*, 2005)  $k = 6 \times 10^8 \text{ M}^{-1} \text{ s}^{-1}$ ) were spiked into phenol solution before pumping into the electrochemical filter. Scavenger tests showed that phenol oxidation was mainly due to oxidation by  $\text{H}_2\text{O}_2$ . Compared with the control without the scavenger, phenol oxidation rate decreased by 24% after benzoquinone was introduced at the start of the filtration (0 s) or after the system was operated for 540 s, suggest that  $\text{O}_2^{\bullet-}$  contributed to partial phenol oxidation in the electrochemical CNT filter (Figure 5-10). Conversely, no significant change in the phenol oxidation rate was observed when *tert*-butanol was spiked, indicating that phenol oxidation by  $\text{OH}^{\bullet}$  was negligible within the electrochemical CNT filter (Figure 5-11). Therefore, more than 87% of phenol oxidation can be mainly attributed to direct oxidation by  $\text{H}_2\text{O}_2$  or indirect oxidation by other reactive oxygen species (e.g.,  $\text{O}_2^{\bullet-}$  and  $\text{HO}_2^{\bullet}$ ) produced at during the filtration.

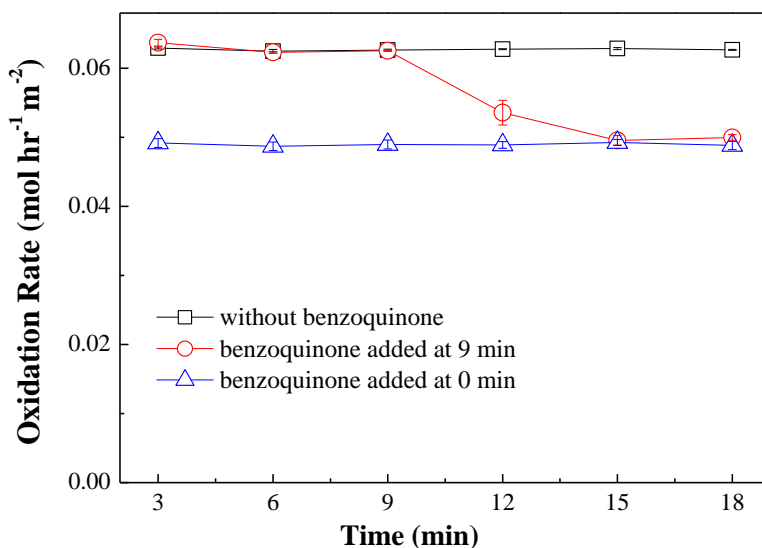


**Figure 5-10. Effect of benzoquinone on phenol oxidation rate**  
 Experimental conditions: Applied cathode potential = -0.4 V vs. Ag/AgCl,  $[\text{Na}_2\text{SO}_4] = 10 \text{ mmol L}^{-1}$ , flow rate =  $1.5 \text{ mL min}^{-1}$ .

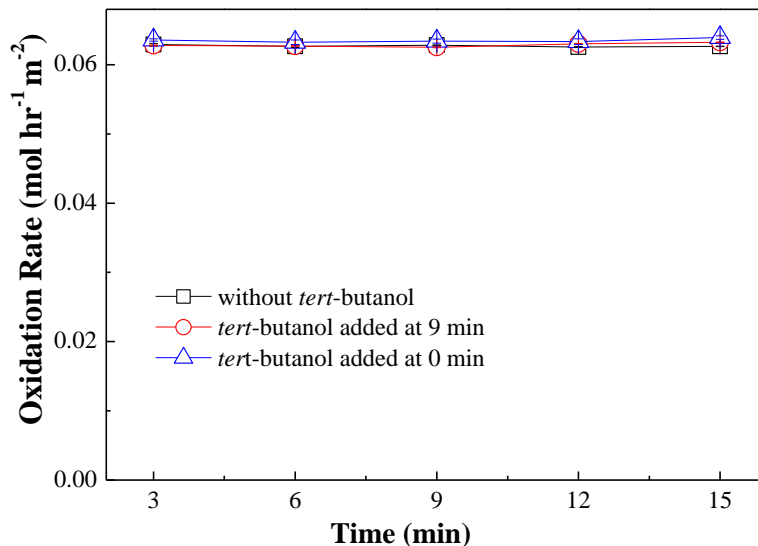


**Figure 5-11. Effect of *tert*-butanol on phenol oxidation rate**  
 Experimental conditions: Applied cathode potential = -0.4 V vs. Ag/AgCl, [Na<sub>2</sub>SO<sub>4</sub>] = 10 mmol L<sup>-1</sup>, flow rate = 1.5 mL min<sup>-1</sup>.

## 5.9 Phenol removal effect in long term

As the electrochemical removal of phenol may decrease due to reduced reactive CNT surface sites that were consumed by adsorbed compounds or oxidation by-products, a continuous operation of 4 h was conducted to evaluate phenol removal and long-term stability of the system at conditions with flow rate 1.5 mL min<sup>-1</sup>, 50 mg L<sup>-1</sup> influent phenol, 44 mg L<sup>-1</sup> DO and -0.4 V cathode potential. Although some polymerization was observed on CNT surface (Figure 5-12), CNT membrane performed pretty stably for 4 hours, an average phenol oxidation rate of 0.059 ± 0.001 mol hr<sup>-1</sup> m<sup>-2</sup> and phenol removal efficiency of 87 ± 1.8% were achieved after 4 h of continuous operation under an applied cathode potential of -0.4 V (vs. Ag/AgCl) (Figure 5-13). The current decreased slightly from 5.6 mA at the beginning to 4.5 mA at 240 minutes. The high oxidation rates and removal efficiency and absence of

complete breakthrough indicated that the primary removal mechanism of phenol was oxidation, rather than physical adsorption.

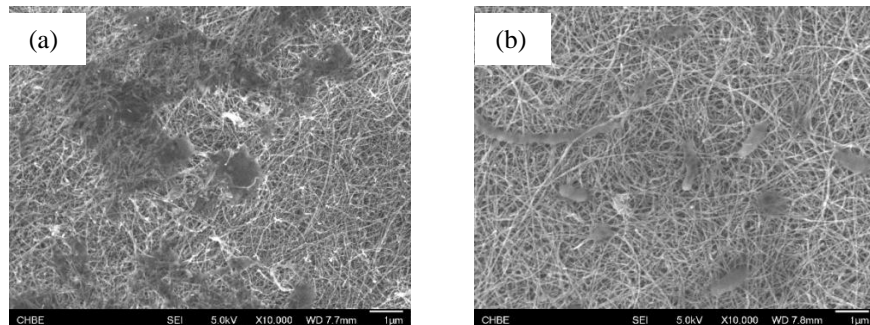


**Figure 5-12. FESEM images of (a) cathodic and (b) anodic CNT filters after 4 h continuous phenol oxidation, showing some polymerization on CNT surface.**

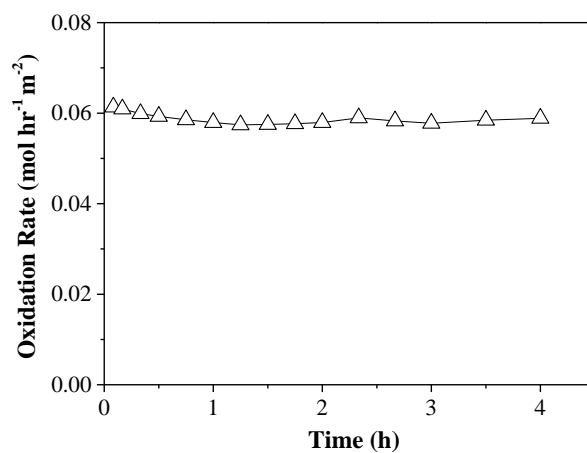


**Figure 5-13. Phenol oxidation rate and current as a function of time**  
Experimental conditions: [Phenol]<sub>IN</sub> = 50 mg L<sup>-1</sup>, applied cathode potential = -0.4 V vs. Ag/AgCl, [Na<sub>2</sub>SO<sub>4</sub>] = 10 mmol L<sup>-1</sup>, flow rate = 1.5 mL min<sup>-1</sup>.

## **6 ENERGY EFFICIENCY AND APPLICATION FOR THE ELECTROCHEMICAL CARBON NANOTUBES FILTER SYSTEM**

### **6.1 Energy consumption for electrochemical phenol filtration**

The energy consumption for electrochemical phenol filtration is calculated at an optimized total cell potential of 1.85 V (corresponds to a cathode potential of -0.4 V vs. Ag/AgCl) by assuming 28 electrons transferred per phenol molecule to be 3.75 kW hr kg<sup>-1</sup> COD. Additionally, the liquid needs to be pumped through the filter, and therefore the pumping energy should also be considered. For a common back pressure is 15 kPa (Gao & Vecitis, 2011) at a flow rate of 1.5 mL min<sup>-1</sup> and a pump efficiency of 75%, the total energy cost for pumping is 1.35 J (Liu & Vecitis, 2012), which is only 2.2% of the energy used for electrochemical H<sub>2</sub>O<sub>2</sub> production (total cell potential of 1.85 V and current of 9.05 mA). These values are comparative to or lower than state-of-the-art electrochemical oxidation processes with energy consumptions in the range of 5-100 kW hr kg<sup>-1</sup> COD (Panizza & Cerisola, 2009). The efficient oxidation rates of phenol revealed that H<sub>2</sub>O<sub>2</sub> production coupled with electrochemical CNT filters could be used to efficiently remove phenolic compounds in wastewater.

Although there was additional electrical energy input in the filtration system, the low applied potential, high H<sub>2</sub>O<sub>2</sub> yield, high removal efficiency, short residence time, and long service time can compensate this additional energy input. Furthermore, a solar panel can be used to provide low potential so electrochemical CNT filters may be widely used as a cost-effective point-of-use treatment system. Overall, the results presented here quantitatively exemplify some of the advantages of using a 3D electrode

in the flow-through configuration and demonstrate the potential of a CNT electrochemical filter for environmental applications and investigations are currently underway to better understand and to further optimize the electrochemical filtration process coupled with *in situ* generated H<sub>2</sub>O<sub>2</sub>.

## 6.2 Oxidation of other organic contaminants

The effective removal of phenol has revealed the potential to use such electrochemical filter for water purification. To further study the efficiency of using this electrochemical system for organic oxidation, the filter was tested with three additional organic compounds: tetracycline (typical PPCP), methyl orange (typical azo-dye), and geosmin (typical off-flavor compound). The initial concentrations of tetracycline, methyl orange, and geosmin were 0.1 mmol L<sup>-1</sup>, 0.1 mmol L<sup>-1</sup>, and 0.55 nmol L<sup>-1</sup>, respectively (Figure 6-1). For all three organic compounds, efficient removal were obtained under optimized conditions (i.e., applied cathode potential = -0.4 V vs. Ag/AgCl, DO = 44 mg L<sup>-1</sup>, pH = 6.46) with efficiency above 87.4%, indicating that such electrochemical filters were highly efficient for water purification.

For the system, effective removal efficiency of phenol (87.0±1.8%) was achieved within 4 h of continuous operation at optimized potential of -0.4 V (vs. Ag/AgCl). For future improvements on phenol removal efficiency in this field, several methods could be used to enhance phenol removal effect: prepare more amount of CNT particles for each membrane, which will increase reaction area and improve efficiency; select an electrolyte with better electron transference, enhancing electrooxidation efficiency; combine photochemical catalysis with electrochemical technology in the system. These methods should be studied in future research to improve phenol removal efficiency.

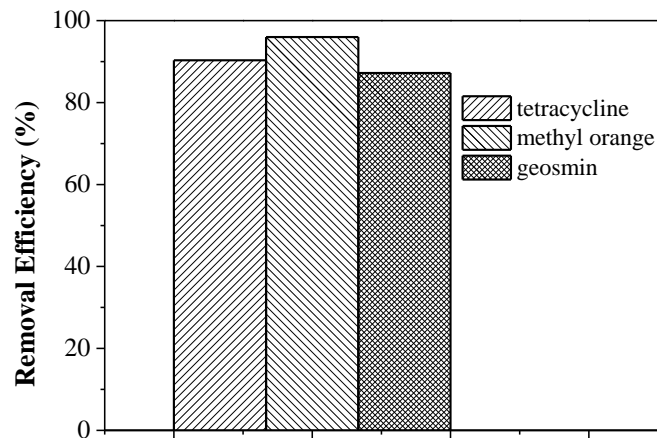


**Figure 6-1. Comparison of removal efficiency of  $0.1 \text{ mmol L}^{-1}$  tetracycline,  $0.1 \text{ mmol L}^{-1}$  methyl orange and  $0.55 \text{ nmol L}^{-1}$  geosmin by the electrochemical filtration system.**

Experimental conditions: applied cathode potential =  $-0.4 \text{ V vs. Ag/AgCl}$ ,  $[\text{Na}_2\text{SO}_4] = 10 \text{ mmol L}^{-1}$ ,  $\text{DO} = 44 \text{ mg L}^{-1}$ , flow rate =  $1.5 \text{ mL min}^{-1}$ .

## 7 CONCLUSIONS AND RECOMMENDATIONS

### 7.1 Conclusions

(1) Aqueous phenol could be degraded by electrochemical filtration system with carbon nanotube through absorption and oxidation. The removal effect, 87%, could be maintained for at least 4 hours from the results of experiment.

(2) Many factors would affect  $\text{H}_2\text{O}_2$  production, such as cathode materials, applied potential, flow rate, pH, and DO concentrations. The optimized conditions for the filtration system include -0.4 V cathode potential, C grade CNT membranes treated with calcination and hydrogen chloride acid,  $1.5 \text{ mL min}^{-1}$  flow rate, neutral pH value (pH = 6.46) and  $44 \text{ mg L}^{-1}$  dissolved oxygen in influent solution. Hydrogen peroxide was generated in system with the rate of  $1.4 \text{ mol L}^{-1} \text{ m}^{-2}$  at optimized conditions.

(3) Breakthrough of  $50 \text{ mg L}^{-1}$  phenol occurred in less than 30 min by CNT sorption. An influent concentration of  $50 \text{ mg L}^{-1}$  phenol was oxidized at the rate of  $0.06 \text{ mol hr}^{-2} \text{ m}^{-2}$  at optimized conditions with 92% aqueous phenol was removed from influent solutions. Molecular phenol was mostly destroyed within the short residence time ( $\sim 1\text{s}$ ) and oxidized into  $\text{CO}_2$  induced from high TOC removal efficiency (over 90%).

(4) Besides phenol, methyl orange, tetracycline and geosmin were studied for their removal efficiency with the electrochemical system. For all three compounds, their efficiency for removal were above 87.4% with initial concentration of  $0.1 \text{ mmol L}^{-1}$  tetracycline,  $0.1 \text{ mmol L}^{-1}$  methyl orange, and  $0.55 \text{ nmol L}^{-1}$  geosmin.

## 7.2 Recommendations

Although high hydrogen peroxide production and phenol removal efficiency were achieved in the electrochemical filtration system, several disadvantages limited further utilization of this innovative technology. For industrial utilization, a higher influent concentration of organic compounds would be treated; the system should run for a longer term to test its robustness and stability. The performance of H<sub>2</sub>O<sub>2</sub> generation and organic compounds removal should be tested after scaling up of the system. Phenol oxidation products should be further studied to ensure no toxic productions in effluent water.



## 8 BIBLIOGRAPHY

- Agladze, G. R., Tsurtsunia, G. S., Jung, B. I., Kim, J. S., & Gorelishvili, G. (2007). Comparative study of hydrogen peroxide electro-generation on gas-diffusion electrodes in undivided and membrane cells. *Journal of Applied Electrochemistry*, 37(3), 375-383. doi: 10.1007/s10800-006-9269-x
- Agladze, GR, Tsurtsunia, GS, Jung, B-I, Kim, J-S, & Gorelishvili, G. (2007). Comparative study of hydrogen peroxide electro-generation on gas-diffusion electrodes in undivided and membrane cells. *Journal of Applied Electrochemistry*, 37(3), 375-383.
- The ATSDR 2011 Substance Priority List. (2011). from <http://www.atsdr.cdc.gov/spl/>.
- Bacon, Roger. (2004). Growth, structure, and properties of graphite whiskers. *Journal of Applied Physics*, 31(2), 283-290.
- Baughman, Ray H, Zakhidov, Anvar A, & de Heer, Walt A. (2002). Carbon nanotubes--the route toward applications. *Science*, 297(5582), 787-792.
- Beckett, Michael A., & Hua, Inez. (2001). Impact of Ultrasonic Frequency on Aqueous Sonoluminescence and Sonochemistry. *J. Phys. Chem. A*, 105(15), 3796-3802.
- Bellamy, William D, Hickman, Gary T, Mueller, Paul A, & Ziemba, Neil. (1991). Treatment of VOC-contaminated groundwater by hydrogen peroxide and ozone oxidation. *Research Journal of the Water Pollution Control Federation*, 120-128.
- Bethune, DS, Klang, CH, De Vries, MS, Gorman, G, Savoy, R, Vazquez, J, & Beyers, R. (1993). Cobalt-catalysed growth of carbon nanotubes with single-atomic-layer walls.
- Bielski, B. H. J., Cabelli, D. E., Arudi, R. L., & Ross, A. B. (1985). Reactivity of HO<sub>2</sub>/O<sub>2</sub><sup>-</sup> radicals in aqueous solution *J. Phys. Chem. Ref. Data*, 14(4), 1041-1100.
- Brillas, E., Sires, I., & Oturan, M. A. (2009a). Electro-Fenton process and related electrochemical technologies based on Fenton's reaction chemistry. *Chem. Rev.*, 109, 6570-6631.

- Brillas, E., Sires, I., & Oturan, M. A. (2009b). Electro-Fenton process and Related Electrochemical Technologies Based on Fenton's Reaction Chemistry. *Chem. Rev*, *109*, 6570-6631.
- Brillas, Enric, Calpe, Juan C, & Casado, Juan. (2000). Mineralization of 2, 4-D by advanced electrochemical oxidation processes. *Water Research*, *34*(8), 2253-2262.
- Brillas, Enrique, Bastida, Rosa Maria, & Llosa, Elisabet. (1995). Electrochemical destruction of aniline and 4-chloroaniline for waste water treatment using a carbone-PTFE electrode. *J. Electrochem. Soc.*, *142*(6), 1733-1741.
- Buxton, G. V., Greenstock, C. L., Helman, W. Phillip, & Ross, A. B. (1988). Critical review of rate constants for reactions of hydrated electrons, hydrogen atoms and hydroxyl radicals (.OH/.O) in aqueous solution. *J. Phys. Chem. Ref. Data*, *17*(2), 513-886.
- C Kormann, D W Bahnemann, M R Hoffmann. (1988). Photocatalytic production of hydrogen peroxides and organic peroxides in aqueous suspensions of titanium dioxide, zinc oxide, and desert sand. *Environ. Sci. Technol.*, *22*(7), 798-806.
- Calle, Eugenia E, Mervis, Cynthia A, Thun, Michael J, Rodriguez, Carmen, Wingo, Phyllis A, & Heath, Clark W. (1996). Diethylstilbestrol and risk of fatal breast cancer in a prospective cohort of US women. *American journal of epidemiology*, *144*(7), 645-652.
- Cao, Jien, Wang, Qian, Rolandi, Marco, & Dai, Hongjie. (2004). Aharonov-Bohm interference and beating in single-walled carbon-nanotube interferometers. *Physical review letters*, *93*(21), 216803.
- Chakraborty, S, Bhattacharya, T, Patel, TN, & Tiwari, KK. (2010). Biodegradation of phenol by native microorganisms isolated from coke processing wastewater. *Journal of Environmental Biology*, *31*(3).
- Cinke, Martin, Li, Jing, Chen, Bin, Cassell, Alan, Delzeit, Lance, Han, Jie, & Meyyappan, M. (2002). Pore structure of raw and purified HiPco single-walled carbon nanotubes. *Chemical Physics Letters*, *365*(1), 69-74.
- Coleman, Jonathan N., Khan, Umar, Blau, Werner J., & Gun'ko, Yurii K. (2006). Small but strong: A review of the mechanical properties of carbon nanotube-

- polymer composites. *Carbon*, 44(9), 1624-1652. doi:  
10.1016/j.carbon.2006.02.038
- Collins, Philip G, & Avouris, Phaedon. (2000). Nanotubes for electronics. *Scientific American*, 283(6), 62-69.
- Cottrell, AH. (1964). Strong solids. *Proceedings of the Royal Society of London. Series A. Mathematical and Physical Sciences*, 282(1388), 2-9.
- Dai, Jiayin, Xu, Muqi, Chen, Jiping, Yang, Xiangping, & Ke, Zhenshan. (2007). PCDD/F, PAH and heavy metals in the sewage sludge from six wastewater treatment plants in Beijing, China. *Chemosphere*, 66(2), 353-361.
- De Grey, A. D. (2002). HO<sub>2</sub>\*: the forgotten radical. *DNA Cell Biol.*, 21(4), 251-257. doi: 10.1089/104454902753759672
- Do, J. S., & Chen, C. P. (1993). In situ oxidative degradation of formaldehyde with electrogenerated hydrogen peroxide. *J. Electrochem. Soc.*, 140(6), 1632-1637.
- Forti, J. C., Nunes, J. A., Lanza, M. R. V., & Bertazzoli, R. (2007). Azobenzene-modified oxygen-fed graphite/PTFE electrodes for hydrogen peroxide synthesis. *Journal of Applied Electrochemistry*, 37(4), 527-532. doi: 10.1007/s10800-006-9285-x
- Gallegos, Alberto Alvarez, Garc ía, Yary Vergara, & Zamudio, Alvaro. (2005). Solar hydrogen peroxide. *Solar energy materials and solar cells*, 88(2), 157-167.
- Gao, G. D., & Vecitis, C. D. (2011). Electrochemical carbon nanotube filter oxidative performance as a function of surface chemistry. *Environ. Sci. Technol.*, 45(22), 9726-9734. doi: 10.1021/es202271z
- Gao, G., & Vecitis, C. D. (2011). Electrochemical carbon nanotube filter oxidative performance as a function of surface chemistry. *Environ Sci Technol*, 45(22), 9726-9734. doi: 10.1021/es202271z
- Gao, G., & Vecitis, C. D. (2012). Doped carbon nanotube networks for electrochemical filtration of aqueous phenol: electrolyte precipitation and phenol polymerization. *ACS Appl Mater Interfaces*, 4(3), 1478-1489. doi: 10.1021/am2017267
- Gao, Guandao, & Vecitis, Chad D. (2013). Electrocatalysis aqueous phenol with carbon nanotubes networks as anodes: Electrodes passivation and regeneration

- and prevention. *Electrochimica Acta*, 98, 131-138. doi: 10.1016/j.electacta.2013.02.127
- Guillet, N., Roué L., Marcotte, S., Villers, D., Dodelet, J. P., Chhim, N., & Vin, S. Tré (2006). Electrogenation of Hydrogen Peroxide in Acid Medium using Pyrolyzed Cobalt-based Catalysts: Influence of the Cobalt Content on the Electrode Performance. *Journal of Applied Electrochemistry*, 36(8), 863-870. doi: 10.1007/s10800-005-7174-3
- Haag, W. R., & David Yao, C. C. (1992). Rate constants for reaction of hydroxyl radicals with several drinking water contaminants. *Environ. Sci. Technol.*, 26(5), 1005-1013.
- Hafner, Jason H, Cheung, Chin-Li, Oosterkamp, Tjerk H, & Lieber, Charles M. (2001). High-yield assembly of individual single-walled carbon nanotube tips for scanning probe microscopies. *The Journal of Physical Chemistry B*, 105(4), 743-746.
- Harrison, Ellen Z, Oakes, Summer Rayne, Hysell, Matthew, & Hay, Anthony. (2006). Organic chemicals in sewage sludges. *Science of the total environment*, 367(2), 481-497.
- Hong, Seunghun, & Myung, Sung. (2007). A flexible approach to mobility. *Nature Nanotech*, 2, 207-208.
- Hsiao, Y. L., & Nobe, K. (1993). Oxidative Reactions of Phenol and Chlorobenzene with in Situ Electrogenerated Fenton's Reagent. *Chemical Engineering Communications*, 126(1), 97-110. doi: 10.1080/00986449308936212
- Iijima, Sumio. (1991). Helical microtubules of graphitic carbon. *nature*, 354(6348), 56-58.
- Iijima, Sumio, & Ichihashi, Toshinari. (1993). Single-shell carbon nanotubes of 1-nm diameter.
- Isarain-Chávez, E., Rosa, C. de la, Martínez-Huitle, C. A., & Peralta-Hernández, J. M. (2013). On-site Hydrogen Peroxide Production at Pilot Flow Plant. *Int. J. Electrochem. Sci.*, 8, 3084-3094.

- Jacobs, Lee W, O'Connor, GA, Overcash, MA, Zabik, MJ, & Rygiewicz, P. (1987). Effects of trace organics in sewage sludges on soil-plant systems and assessing their risk to humans.
- Khataee, A. R., Safarpour, M., Zarei, M., & Aber, S. (2011). Electrochemical generation of H<sub>2</sub>O<sub>2</sub> using immobilized carbon nanotubes on graphite electrode fed with air: Investigation of operational parameters. *Journal of Electroanalytical Chemistry*, 659(1), 63-68. doi: 10.1016/j.jelechem.2011.05.002
- Kolpin, Dana W, Furlong, Edward T, Meyer, Michael T, Thurman, E Michael, Zaugg, Steven D, Barber, Larry B, & Buxton, Herbert T. (2002). Pharmaceuticals, hormones, and other organic wastewater contaminants in US streams, 1999-2000: A national reconnaissance. *Environmental science & technology*, 36(6), 1202-1211.
- Kornienko, G. V., Chaenko, N. V., eva, I. S. Vasil', & Kornienko, V. L. (2004). Indirect electrooxidation of organic substrates by hydrogen peroxide generated in an oxygen gas-diffusion electrode. *Russ. J. Electrochem.*, 40(2), 148-152.
- Kornienko, VL, & Kolyagin, GA. (2003). Indirect oxidation of organic substances by intermediates of the oxygen reduction. *Russian journal of electrochemistry*, 39(12), 1308-1316.
- Lazarova, Z, & Spendlingwimmer, R. (2008). Treatment of yellow water by membrane separations and advanced oxidation methods. *Water Science & Technology*, 58(2).
- Lee, Sang Moon, Lee, Soon Chang, Jung, Jong Hwa, & Kim, Hae Jin. (2005). Pore characterization of multi-walled carbon nanotubes modified by KOH. *Chem. Phys. Lett.*, 416(4-6), 251-255.
- Lewis, S. C., Datta, S., Gui, M. H., Coker, E. L., Huggins, F. E., Dauner, S., . . . Bhattacharyya, D. (2011). Reactive nanostructured membranes for water purification. *PNAS*, 108(21), 8577-8582. doi: 10.1073/pnas.1101144108/-/DCSupplemental

- Li, Hui, Liu, Hao, Jong, Zöe, Qu, Wei, Geng, Dongsheng, Sun, Xueliang, & Wang, Haijiang. (2011). Nitrogen-doped carbon nanotubes with high activity for oxygen reduction in alkaline media. *International Journal of Hydrogen Energy*, 36(3), 2258-2265. doi: 10.1016/j.ijhydene.2010.11.025
- Liu, H., & Vecitis, C. D. (2012). Reactive transport mechanism for organic oxidation during electrochemical filtration: Mass-transfer, physical adsorption, and electron-transfer. *J. Phys. Chem. C*, 116(1), 374-383. doi: 10.1021/jp209390b
- Liu, Han, & Vecitis, Chad D. (2012). Reactive Transport Mechanism for Organic Oxidation during Electrochemical Filtration: Mass-Transfer, Physical Adsorption, and Electron-Transfer. *The Journal of Physical Chemistry C*, 116(1), 374-383. doi: 10.1021/jp209390b
- Liu, Y., Li, J., Zhou, B., Li, X., Chen, H., Chen, Q., . . . Cai, W. (2011). Efficient electricity production and simultaneously wastewater treatment via a high-performance photocatalytic fuel cell. *Water Research*, 45(13), 3991-3998. doi: 10.1016/j.watres.2011.05.004
- Ma, J., Sui, M., Zhang, T., & Guan, C. (2005). Effect of pH on MnO<sub>x</sub>/GAC catalyzed ozonation for degradation of nitrobenzene. *Water Res.*, 39(5), 779-786. doi: 10.1016/j.watres.2004.11.020
- Ma, R. Z., Xu, C. L., Wei, B. Q., Liang, J., Wu, D. H., & Li, D. J. (1999). Electrical conductivity and field emission characteristics of hot-pressed sintered carbon nanotubes. *Mater. Res. Bull.*, 34(5), 741-747. doi: [http://dx.doi.org/10.1016/S0025-5408\(99\)00064-1](http://dx.doi.org/10.1016/S0025-5408(99)00064-1)
- Oki, Taikan, & Kanae, Shinjiro. (2006). Global hydrological cycles and world water resources. *science*, 313(5790), 1068-1072.
- Olaniran, A. O., & Igbinsola, E. O. (2011). Chlorophenols and other related derivatives of environmental concern: Properties, distribution and microbial degradation processes. *Chemosphere*, 83(10), 1297-1306. doi: 10.1016/j.chemosphere.2011.04.009
- Oshitani, N., Kitano, A., Okabe, H., Nakamura, S., Matsumoto, T., & Kobayashi, K. (1993). Location of superoxide anion generation in human colonic mucosa obtained by biopsy. *Gut.*, 34(7), 936-938.

- Pan, B., & Xing, B. (2008). Adsorption mechanisms of organic chemicals on carbon nanotubes. *Environ. Sci. Technol.*, 42(24), 9005-9013. doi: 10.1021/es801777n
- Panizza, M., & Cerisola, G. (2009). Direct and mediated anodic oxidation of organic pollutants. *Chem. Rev.*, 109(12), 6541-6569. doi: 10.1021/cr9001319
- Panizza, Marco, & Cerisola, Giacomo. (2008). Electrochemical generation of H<sub>2</sub>O<sub>2</sub> in low ionic strength media on gas diffusion cathode fed with air. *Electrochimica Acta*, 54(2), 876-878.
- Pelegrini, RT, Freire, RS, Duran, N, & Bertazzoli, R. (2001). Photoassisted electrochemical degradation of organic pollutants on a DSA type oxide electrode: process test for a phenol synthetic solution and its application for the E1 bleach kraft mill effluent. *Environmental science & technology*, 35(13), 2849-2853.
- Peng, Bei, Locascio, Mark, Zapol, Peter, Li, Shuyou, Mielke, Steven L, Schatz, George C, & Espinosa, Horacio D. (2008). Measurements of near-ultimate strength for multiwalled carbon nanotubes and irradiation-induced crosslinking improvements. *Nature nanotechnology*, 3(10), 626-631.
- Pignatello, Joseph J., Oliveros, Esther, & MacKay, Allison. (2006a). Advanced Oxidation Processes for Organic Contaminant Destruction Based on the Fenton Reaction and Related Chemistry. *Critical Reviews in Environmental Science and Technology*, 36(1), 1-84. doi: 10.1080/10643380500326564
- Pignatello, Joseph J., Oliveros, Esther, & MacKay, Allison. (2006b). Advanced oxidation processes for organic contaminant destruction based on the Fenton reaction and related chemistry. *Crit. Rev. Environ. Sci. Technol.*, 36(1), 1-84. doi: 10.1080/10643380500326564
- Pletcher, Derek. (1999). Indirect Oxidations Using Electrogenerated Hydrogen Peroxide. *Acta. Chem. Scand.*, 53, 745-750.
- Pop, Eric, Mann, David, Wang, Qian, Goodson, Kenneth, & Dai, Hongjie. (2006). Thermal conductance of an individual single-wall carbon nanotube above room temperature. *Nano Letters*, 6(1), 96-100.

- Popov, M, Kyotani, M, Nemanich, RJ, & Koga, Y. (2002). Superhard phase composed of single-wall carbon nanotubes. *Physical Review B*, 65(3), 033408.
- Programme, World Water Assessment. (2009). *Water in a changing world* (Vol. 2): Unesco.
- Qiang, Z. M., Chang, J. H., & Huang, C. P. (2002). Electrochemical generation of hydrogen peroxide from dissolved oxygen in acidic solutions. *Water Res.*, 36(1), 85-94. doi: [http://dx.doi.org/10.1016/S0043-1354\(01\)00235-4](http://dx.doi.org/10.1016/S0043-1354(01)00235-4)
- Qiang, Zhimin, Chang, Jih-Hsing, & Huang, Chin-Pao. (2002). Electrochemical generation of hydrogen peroxide from dissolved oxygen in acidic solutions. *Water Research*, 36(1), 85-94.
- Qiao, Jun-Qin, Yuan, Na, Tang, Chang-Jin, Yang, Jing, Zhou, Jian, Lian, Hong-Zhen, & Dong, Lin. (2012). Determination of catalytic oxidation products of phenol by RP-HPLC. *Research on Chemical Intermediates*, 38(2), 549-558.
- Radjenović, J, Petrović, M, Ventura, F, & Barceló, D. (2008). Rejection of pharmaceuticals in nanofiltration and reverse osmosis membrane drinking water treatment. *Water Research*, 42(14), 3601-3610.
- Rahaman, M. S., Vecitis, C. D., & Elimelech, M. (2012). Electrochemical carbon-nanotube filter performance toward virus removal and inactivation in the presence of natural organic matter. *Environmental Science and Technology*, 46(3), 1556-1564. doi: 10.1021/es203607d
- Richardson, S. D., & Ternes, T. A. (2011). Water analysis: emerging contaminants and current issues. *Anal Chem*, 83(12), 4614-4648. doi: 10.1021/ac200915r
- Sanderson, M, Williams, MA, Daling, JR, Holt, VL, Malone, KE, Self, SG, & Moore, DE. (1998). Maternal factors and breast cancer risk among young women. *Paediatric and perinatal epidemiology*, 12, 397-407.
- Sawada, Y., Iyanagi, T., & Yamazaki, I. (1975). Relation between redox potentials and rate constants in reactions coupled with the system oxygen-superoxide. *Biochem.*, 14(17), 3761-3764.
- Schnoor, M. H., & Vecitis, C. D. (2013). Quantitative examination of aqueous ferrocyanide oxidation in a carbon nanotube electrochemical filter: Effects of



- flow rate, ionic strength, and cathode material. *J. Phys. Chem. C*, 117(6), 2855-2867. doi: 10.1021/jp3112099
- Schwarzenbach, René P, Egli, Thomas, Hofstetter, Thomas B, Von Gunten, Urs, & Wehrli, Bernhard. (2010). Global water pollution and human health. *Annual Review of Environment and Resources*, 35, 109-136.
- Scialdone, Onofrio, Galia, Alessandro, & Sabatino, Simona. (2013). Electro-generation of H<sub>2</sub>O<sub>2</sub> and abatement of organic pollutant in water by an electro-Fenton process in a microfluidic reactor. *Electrochemistry Communications*, 26, 45-47. doi: 10.1016/j.elecom.2012.10.006
- Shaegh, Seyed Ali Mousavi, Ehteshami, Seyyed Mohsen Mousavi, & Hwa Chan, Siew. (2012). A membraneless hydrogen peroxide fuel cell using Prussian Blue as cathode material. *Energy & Environmental Science*, 5(8), 8225-8228.
- Sirés, Ignasi, & Brillas, Enric. (2012). Remediation of water pollution caused by pharmaceutical residues based on electrochemical separation and degradation technologies: A review. *Environment International*, 40, 212-229. doi: 10.1016/j.envint.2011.07.012
- Smith, SR. (2000). Are controls on organic contaminants necessary to protect the environment when sewage sludge is used in agriculture? *Progress in Environmental Science*, 2(2), 129-146.
- Sudoh, Masao, Kodera, Takamasa, SAKAI, KUNIO, ZHANG, JIN QUAN, & KOIDE, Kozo. (1986). Oxidative degradation of aqueous phenol effluent with electrogenerated Fenton's reagent. *Journal of chemical engineering of japan*, 19(6), 513-518.
- Tang, ZK, Zhang, Lingyun, Wang, N, Zhang, XX, Wen, GH, Li, GD, . . . Sheng, Ping. (2001). Superconductivity in 4 angstrom single-walled carbon nanotubes. *Science*, 292(5526), 2462-2465.
- Taylor, Brynn, Skelly, David, Demarchis, Livia K, Slade, Martin D, Galusha, Deron, & Rabinowitz, Peter M. (2005). Proximity to pollution sources and risk of amphibian limb malformation. *Environmental Health Perspectives*, 113(11), 1497.

- Thorpe, G. W., Reodica, M., Davies, M. J., Heeren, G., Jarolim, S., Pillay, B., . . . Dawes, I. W. (2013). Superoxide radicals have a protective role during H<sub>2</sub>O<sub>2</sub> stress. *Mol. Biol. Cell*, 24(18), 2876-2884. doi: 10.1091/mbc.E13-01-0052
- Thostenson, Erik T, Li, Chunyu, & Chou, Tsu-Wei. (2005). Nanocomposites in context. *Composites Science and Technology*, 65(3), 491-516.
- Vahid, Behrouz, & Khataee, Alireza. (2013). Photoassisted electrochemical recirculation system with boron-doped diamond anode and carbon nanotubes containing cathode for degradation of a model azo dye. *Electrochimica Acta*, 88, 614-620.
- Vecitis, C. D., Gao, G., & Liu, H. (2011a). Electrochemical carbon nanotube filter for adsorption, desorption, and oxidation of aqueous dyes and anions. *J. Phys. Chem. C*, 115(9), 3621-3629. doi: 10.1021/jp111844j
- Vecitis, C. D., Gao, G., & Liu, H. (2011b). Electrochemical carbon nanotube filter for adsorption, desorption, and oxidation of aqueous dyes and anions. *J. Phys. Chem. C*, 115(9), 3621-3629. doi: 10.1021/jp111844j
- Vecitis, C. D., Schnoor, M. H., Rahaman, M. S., Schiffman, J. D., & Elimelech, M. (2011). Electrochemical multiwalled carbon nanotube filter for viral and bacterial removal and inactivation. *Environ Sci Technol*, 45(8), 3672-3679. doi: 10.1021/es2000062
- Vorosmarty, C. J., McIntyre, P. B., Gessner, M. O., Dudgeon, D., Prusevich, A., Green, P., . . . Davies, P. M. (2010). Global threats to human water security and river biodiversity. *Nature*, 467(7315), 555-561. doi: 10.1038/nature09440
- Wilson, John T, Armstrong, John M, & Rifai, HS. (1994). A full-scale field demonstration on the use of hydrogen peroxide for in situ bioremediation of an aviation gasoline-contaminated aquifer. *Bioremediation: Field Experience*, 333-360.
- Wu, Zucheng, & Zhou, Minghua. (2001). Partial degradation of phenol by advanced electrochemical oxidation process. *Environmental science & technology*, 35(13), 2698-2703.

- Xie, Y. B., & Li, X. Z. (2006). Degradation of bisphenol A in aqueous solution by H<sub>2</sub>O<sub>2</sub>-assisted photoelectrocatalytic oxidation. *J Hazard Mater*, 138(3), 526-533. doi: 10.1016/j.jhazmat.2006.05.074
- Xu, Fu-Liu, Jorgensen, Sven Erik, Shimizu, Yoshihisa, & Silow, Eugen. (2013). Persistent Organic Pollutants in Fresh Water Ecosystems. *The Scientific World Journal*, 2013.
- Yang, H. Y., Han, Z. J., Yu, S. F., Pey, K. L., Ostrikov, K., & Karnik, R. (2013). Carbon nanotube membranes with ultrahigh specific adsorption capacity for water desalination and purification. *Nat Commun*, 4, 2220. doi: 10.1038/ncomms3220
- Yang, YZ, Li, YP, Yang, DW, Duan, F, & Cao, HB. (2013). [Degradation of phenol with a Fe/cu-catalytic heterogeneous-Fenton process]. *Huan jing ke xue= Huanjing kexue/[bian ji, Zhongguo ke xue yuan huan jing ke xue wei yuan hui" Huan jing ke xue" bian ji wei yuan hui.]*, 34(7), 2658-2664.
- Yuan, S., Fan, Y., Zhang, Y., Tong, M., & Liao, P. (2011). Pd-catalytic in situ generation of H<sub>2</sub>O<sub>2</sub> from H<sub>2</sub> and O<sub>2</sub> produced by water electrolysis for the efficient electro-fenton degradation of rhodamine B. *Environ Sci Technol*, 45(19), 8514-8520. doi: 10.1021/es2022939
- Zanello, Laura P, Zhao, Bin, Hu, Hui, & Haddon, Robert C. (2006). Bone cell proliferation on carbon nanotubes. *Nano Letters*, 6(3), 562-567.
- Zhang, M., Y. Yan, Gong, K., Mao, L., Z. Guo, & Chen, Y. (2004). Electrostatic Layer-by-Layer Assembled Carbon Nanotube Multilayer Film and Its Electrocatalytic Activity for O<sub>2</sub> Reduction *Langmuir*, 20, 8781-8785.
- Zhang, Q. Y., & Vecitis, C. D. (2014). Conductive CNT-PVDF membrane for capacitive organic fouling reduction. *J. Mem. Sci.*, 459, 143-156. doi: 10.1016/j.memsci.2014.02.017
- Zhang, X., Fu, J., Zhang, Y., & Lei, L. (2008). A nitrogen functionalized carbon nanotube cathode for highly efficient electrocatalytic generation of H<sub>2</sub>O<sub>2</sub> in Electro-Fenton system. *Separation and Purification Technology*, 64(1), 116-123. doi: 10.1016/j.seppur.2008.07.020

- Zhao, X, Liu, Y, Inoue, S, Suzuki, T, Jones, RO, & Ando, Y. (2004). Smallest carbon nanotube is 3 Å in diameter. *Physical review letters*, 92(12), 125502.
- Zhou, M., Yu, Q., & Lei, L. (2008). The preparation and characterization of a graphite–PTFE cathode system for the decolorization of C.I. Acid Red 2. *Dyes Pigments*, 77(1), 129-136. doi: 10.1016/j.dyepig.2007.04.002